

See discussions, stats, and author profiles for this publication at: <https://www.researchgate.net/publication/379084374>

Differential utilisation of subcellular skeletal muscle glycogen pools: a comparative analysis between 1 and 15 min of maximal exercise

Article in *The Journal of Physiology* · March 2024

DOI: 10.1113/JP285762

CITATIONS

0

READS

23

4 authors:



Camilla Schytz

University of Southern Denmark

7 PUBLICATIONS 23 CITATIONS

[SEE PROFILE](#)



Niels Ortenblad

University of Southern Denmark

152 PUBLICATIONS 4,526 CITATIONS

[SEE PROFILE](#)



Kasper Gejl

University of Southern Denmark

37 PUBLICATIONS 652 CITATIONS

[SEE PROFILE](#)



Joachim Nielsen

University of Southern Denmark

72 PUBLICATIONS 2,785 CITATIONS

[SEE PROFILE](#)

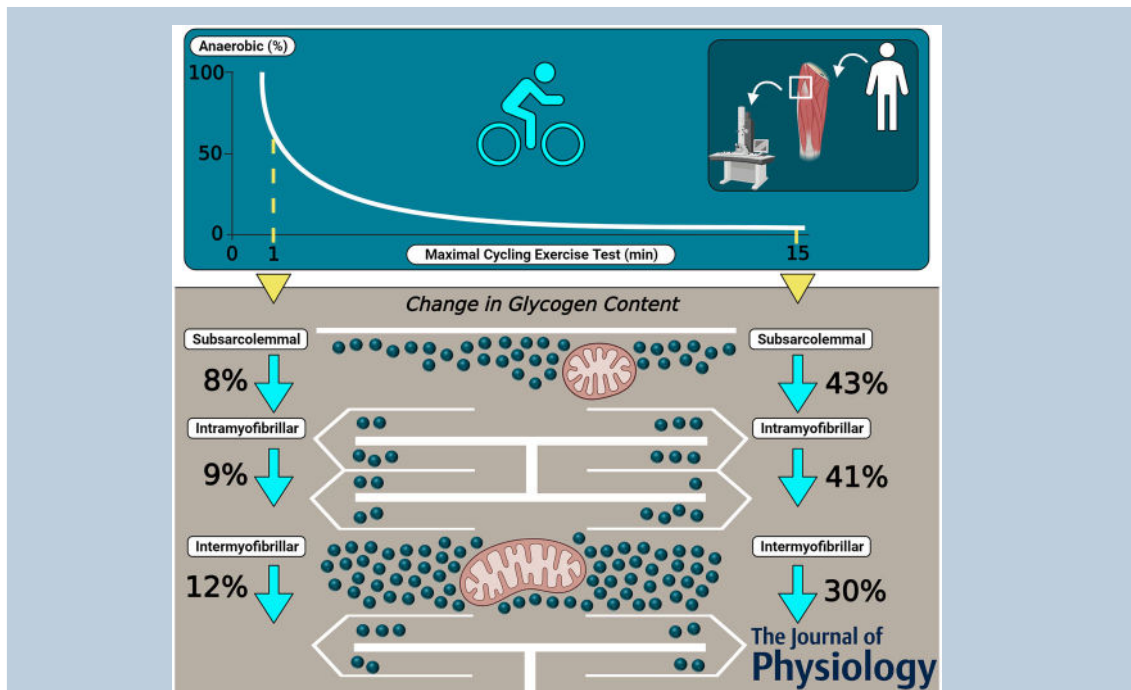
Differential utilisation of subcellular skeletal muscle glycogen pools: a comparative analysis between 1 and 15 min of maximal exercise

Camilla Tvede Schytz , Niels Ørtenblad , Kasper Degn Gejl  and Joachim Nielsen 

Department of Sports Science and Clinical Biomechanics, Faculty of Health Sciences, University of Southern Denmark, Odense, Denmark

Handling Editors: Paul Greenhaff & Bruno Grassi

The peer review history is available in the Supporting Information section of this article (<https://doi.org/10.1113/JP285762#support-information-section>).



Abstract In skeletal muscle, glycogen particles are distributed both within and between myofibrils, as well as just beneath the sarcolemma. Their precise localisation may influence their degradation rate. Here, we investigated how exercise at different intensities and durations (1- and 15-min maximal exercise) with known variations in glycogenolytic rate and contribution from anaerobic metabolism affects utilisation of the distinct pools. Furthermore, we investigated how decreased glycogen availability achieved through lowering carbohydrate and energy intake after glycogen-depleting exercise affect the storage of glycogen particles (size, numerical density, localisation). Twenty participants were divided into two groups performing either a 1-min ($n = 10$) or a 15-min ($n = 10$) maximal cycling exercise test. In a randomised, counterbalanced, cross-over design, the exercise tests were performed following short-term consumption of two distinct diets with either high or moderate carbohydrate content (10 vs. 4 g kg⁻¹ body mass (BM) day⁻¹) mediating a difference in total energy consumption (240 vs. 138 g kg⁻¹ BM day⁻¹). Muscle biopsies from m. vastus lateralis were

This article was first published as a preprint. Schytz CT, Ørtenblad N, Gejl KD, Nielsen, J. 2023. Differential utilisation of subcellular skeletal muscle glycogen pools: A comparative analysis between 1 and 15 minutes of maximal exercise. bioRxiv. <https://doi.org/10.1101/2023.09.28.559993>

obtained before and after the exercise tests. Intermyoibrillar glycogen was preferentially utilised during the 1-min test, whereas intramyofibrillar glycogen was preferentially utilised during the 15-min test. Lowering carbohydrate and energy intake after glycogen-depleting exercise reduced glycogen availability by decreasing particle size across all pools and diminishing numerical density in the intramyofibrillar and subsarcolemmal pools. In conclusion, distinct subcellular glycogen pools were differentially utilised during 1-min and 15-min maximal cycling exercise. Additionally, lowered carbohydrate and energy consumption after glycogen-depleting exercise altered glycogen storage by reducing particle size and numerical density, depending on subcellular localisation.

(Received 4 October 2023; accepted after revision 5 March 2024; first published online 19 March 2024)

Corresponding authors C. T. Schytz and J. Nielsen: Department of Sports Science and Clinical Biomechanics, Faculty of Health Sciences, University of Southern Denmark, 5230 Odense M, Denmark. Email: cschytz@health.sdu.dk, jnielsen@health.sdu.dk

Abstract figure legend Distinct subcellular pools of glycogen particles exist within skeletal muscle fibres, distributed both within (intramyofibrillar pool) and between myofibrils (intermyofibrillar pool) as well as just beneath the cellular membrane (subsarcolemmal pool). These pools can be found in proximity to, or at a distance from mitochondria. Their precise localisation may influence their degradation rate during maximal exercise with variations in the contribution of anaerobic energy supply to the total (values in graph based on Gustin (2001)). In the present study we investigated how maximal cycling exercise tests at different intensities and durations (1 and 15 min) with known differences in glycogenolytic rate and in anaerobic energy contribution to total energy turnover (64.6% and 4.5%, respectively) affect utilisation of the subcellular pools of glycogen. In skeletal muscle biopsies from the m. vastus lateralis obtained prior to and after the exercise tests, we show a differential utilisation of the distinct pools. Thus, intermyofibrillar glycogen was preferentially utilised during the 1-min test, whereas intramyofibrillar glycogen was preferentially utilised during the 15-min test. Created in Biorender.com using sources from Biorender.com and own creations.

Key points

- In human skeletal muscle, glycogen particles are localised in distinct subcellular compartments, referred to as intermyofibrillar, intramyofibrillar and subsarcolemmal pools.
- The intermyofibrillar and subsarcolemmal pools are close to mitochondria, while the intramyofibrillar pool is at a distance from mitochondria.
- We show that 1 min of maximal exercise is associated with a preferential utilisation of intermyofibrillar glycogen, and, on the other hand, that 15 min of maximal exercise is associated with a preferential utilisation of intramyofibrillar glycogen.
- Furthermore, we demonstrate that reduced glycogen availability achieved through lowering carbohydrate and energy intake after glycogen-depleting exercise is characterised by a decreased glycogen particle size across all compartments, with the numerical density only diminished in the intramyofibrillar and subsarcolemmal compartments.
- These results suggest that exercise intensity influences the subcellular pools of glycogen differently and that the dietary content of carbohydrates and energy is linked to the size and subcellular distribution of glycogen particles.

Camilla Tvede Schytz has recently finished her PhD studies in exercise physiology at the Department of Sports Science and Clinical Biomechanics, University of Southern Denmark. Her PhD focuses on investigating the acute effects of a carbohydrate and energy manipulation on skeletal muscle glycogen and performance during short-term maximal exercise. Furthermore, characterising human skeletal muscle mitochondria across diverse training statuses and biological sex by combing structural and respiratory measures is another focal point of her PhD. She hopes to continue to conduct research in the future.



Introduction

Glycogen serves as a readily available fuel store in human skeletal muscles, stored as particles mainly in three subcellular localisations: intermyofibrillar, intramyofibrillar and subsarcolemmal (Marchand et al., 2002). These pools differ substantially in capacity, with the intermyofibrillar pool constituting approximately 80% of the total glycogen content, while the intramyofibrillar and subsarcolemmal pools make up between ~5%–15% (Marchand et al., 2002; Nielsen et al., 2011). Despite being the minor pools, intramyofibrillar, and subsarcolemmal glycogen are preferentially used during exhaustive work lasting 4–150 min (Gejl et al., 2017; Jensen, Ørtenblad, et al., 2020; Nielsen et al., 2011), and in three different models we have found that intramyofibrillar glycogen is closely associated with measures of fatigue resistance (Jensen, Ørtenblad, et al., 2020; Nielsen et al., 2009, 2014). However, these observations are based on work performed with a predominantly aerobic metabolism. Considering that the energy yield per glycogen particle significantly diminishes during a shift to anaerobic metabolism (Hargreaves & Spriet, 2018), there exist an unmet need to understand how alterations in the ratio between aerobic and anaerobic metabolism, and herein exercise intensity, affect the utilisation of the different pools of glycogen. Due to possible cytoplasmic diffusion restrictions (Ovadi & Saks, 2004; Verkman, 2002) and based on the topological relationships, where intramyofibrillar glycogen is localised distantly from mitochondria, whereas a large proportion of both intermyofibrillar and subsarcolemmal glycogen particles are situated in close proximity to the mitochondria, a shift from aerobic to anaerobic metabolism may have differential effects on the utilisation of these different pools. Therefore, the first aim of the present study was to investigate the effect of maximal exercise of two different intensities (1 and 15 min maximal cycling exercise) on the utilisation of the three subcellular pools of glycogen.

The volumetric density of skeletal muscle glycogen is a product of particle size and numerical density, which can both be modulated (Marchand et al., 2007). A glycogen particle is a spherical structure, organized in concentric layers (tiers), comprising both branched and unbranched chains of glucose where each chain gives rise to two chains in the following tier except for the outermost chains (Goldsmith et al., 1982; Gunja-Smith et al., 1970; Melendez-Hevia et al., 1993). Importantly, because of this structure, the size of a glycogen particle is self-limiting (Madsen & Cori, 1958) with the estimated highest possible packing density achieved at the 12th tier (Goldsmith et al., 1982; Melendez et al., 1998), resulting in a maximal theoretical diameter of 42 nm (Melendez-Hevia et al.,

1993). Nonetheless, the average size of glycogen particles in human skeletal muscles is submaximal, averaging approximately 25 nm (Gejl et al., 2017; Jensen et al., 2021; Marchand et al., 2002, 2007; Nielsen et al., 2012; Wanson & Drochmans, 1968). In support of a preference for medium-sized particles, the numerical density increases without affecting particle size, when glycogen content is increased by a diet- and exercise-induced supercompensation (Jensen et al., 2021). Conversely, when glycogen content is lowered through a carbohydrate (CHO) restricted diet, the decrease is explained by a reduced numerical density (Jensen et al., 2021). One theory is that medium-sized particles are optimal for degradation rates due to enhanced accessibility for the glycogen degradation enzymes, achieved by both reducing steric hindrance and increasing the surface-to-volume ratio, although it compromises storage efficiency (Shearer & Graham, 2004); however, this remains to be investigated experimentally. Thus, one inherent determinant of glycogen storage (i.e. particle size vs. numerical density) may entail a trade-off between storage efficiency and metabolic power (i.e. particle degradation rate). Another inherent determinant could be the spatial distribution of the particles (Shearer & Graham, 2004) as this may be important to provide a local provision of energy needed due to diffusion restrictions within the cell (Ovadi & Saks, 2004; Verkman, 2002). These inherent factors might influence how dietary CHO and energy consumption affect the glycogen storage pattern. In the previously mentioned study by Jensen et al. (2021), particle sizes in skeletal muscle fibres are remarkably similar across isocaloric diets differing in CHO content (with the low and high CHO condition ingested after glycogen-depleting exercise), but a low CHO diet reduces the numerical density in all pools. Therefore, the second aim of the present study was to investigate how reduced glycogen availability achieved through lowering carbohydrate and energy intake after glycogen-depleting exercise affects the storage of glycogen particles (particle size, numerical density and localisation) within skeletal muscle fibres.

Collectively, the first aim of the present study was to compare the effects of maximal cycling exercise at two different intensities and durations (1 and 15 min) on glycogen volumetric density and subcellular localisation within skeletal muscle fibres, and secondly, in a randomised, counterbalanced, cross-over design to investigate the effects of decreased glycogen availability achieved through short-term lowering of carbohydrate and energy intake following glycogen-depleting exercise on particle size, numerical density and subcellular localisations within skeletal muscle fibres.

Table 1. Participant characteristics

Test	<i>n</i>	Age (years)	Body mass (kg)	Height (m)	$\dot{V}_{O_2\max}$ (ml min ⁻¹ kg ⁻¹ BM)	PO _{max,incremental} (W)
1 min	10	23 (22–26)	78.4 (77.8–79.4)*	1.85 (1.81–1.88)	55.4 (54.1–58.6)*	311 (293–319)
15 min	10	23 (22–23)	74.4 (70.7–77.4)	1.82 (1.80–1.84)	59.3 (55.6–64.2)	307 (275–326)

Values are presented as median (interquartile range).

*Different from 15 min ($P = 0.004$ and $P = 0.049$ for body mass and $\dot{V}_{O_2\max}$, respectively). PO_{max,incremental}, maximal power output.

Methods

Ethical approval

The human skeletal muscle biopsies included in the present study are a part of a larger study (Schytz et al., 2023). This project was approved by The Regional Committees on Health Research Ethics for Southern Denmark (S-20200157) and the experiments conformed to the standards set by the *Declaration of Helsinki* (except for registration in a database). Before providing their written informed consent, the participants were informed about the study and the potential risks and were made aware that they could withdraw from the project at any time.

Participants

For inclusion the participants had to meet the following criteria: male, age 18–40 years, maximal oxygen uptake ($\dot{V}_{O_2\max}$) ≥ 45 ml O₂ min⁻¹ kg⁻¹, engaging in regular endurance training at least 2 times per week, non-vegetarian, non-smoker and otherwise healthy. Twenty recreationally active males meeting these criteria were enrolled in the study and randomly allocated to one of two groups performing either 1 min ($n = 10$) or 15 min ($n = 10$) of maximal cycling exercise (Table 1). Given the time-consuming transmission electron microscopy (TEM) analysis, it was decided before start of the analysis to include only 10 (randomly chosen) of the original 12 participants (Schytz et al., 2023) in the 15-min group due to a weighed and legitimate time consumption for image analyses. Thus, presented values beside TEM-based values are re-calculated from Schytz et al. (2023), due to the lower sample size in the 15-min test of the present study.

Study overview

The twenty participants were randomised to perform tests of either 1 min ($n = 10$) or 15 min ($n = 10$) of maximal

cycling exercise, at the end of two dietary intervention periods. In a randomised and counterbalanced cross-over design, the participants, in each of the 1- and 15-min exercise groups, completed two 5-day intervention periods with glycogen-depleting exercise followed by different CHO consumption strategies with either a high (H-CHO) or a moderate (M-CHO) CHO content (Fig. 1A). The participants consumed the different diets for two full days (Day –1 and –2) in addition to the remainder of the day following the glycogen-depleting exercise on Day –3 (see below). Each intervention period started with a rest day (Day –4) including a diet consisting of a moderate amount of CHO (M-CHO) (4 g kg⁻¹ BM day⁻¹), which was consumed until completion of a glycogen-depleting exercise the following day (Day –3) (Fig. 1A). Hereafter, the participants were randomised in a counterbalanced order to either proceed on the M-CHO diet or to receive a diet containing a high amount of CHO (H-CHO) (10 g kg⁻¹ BM day⁻¹) for the subsequent part of the intervention period (i.e. Day –3 (after glycogen-depleting exercise), –2, and –1). The participants rested the next day (Day –2), and the following day (Day –1) they completed a short training session consisting of cycling exercise. On the final day (Day 0) of each intervention period the participants ingested a standardised breakfast and completed the exercise test (Fig. 1A). These two strategies were separated by 10 days with habitual exercise and diet. Skeletal muscle biopsies were obtained before and immediately after each of the 1-min and 15-min tests (Fig. 1A).

Within each participant, all procedures were performed at the same time of day, on the same weekday, with the same ergometers, and conducted by the same test leader and standardised verbal encouragement in both intervention periods. Experiments were carried out in the laboratories at the Department of Sports Science and Clinical Biomechanics, University of Southern Denmark, Odense.

Diet compositions and control of physical activity level

A detailed description of diets and physical activity level has previously been provided in detail in Schytz et al. (2023). In brief, the diet was strictly controlled in the intervention periods, and two distinct diets, denoted M-CHO and H-CHO, were administered. These diets contained identical amounts of protein, fat and dietary fibres (1.6, 1.0 and 0.4 g kg⁻¹ BM day⁻¹, respectively), but differed with respect to CHO content (M-CHO: 4 g kg⁻¹ BM day⁻¹ vs. H-CHO: 10 g kg⁻¹ BM day⁻¹). This difference in CHO content mediated a lower total

energy content in the M-CHO diet than the H-CHO diet (138 kJ vs. 240 kJ kg⁻¹ BM day⁻¹). The energy content was not balanced between diets to reflect habitual diet compositions applied by athletes in training and prior to competition where protein and fat intake are in agreement with the recommendations from the American College of Sports Medicine (Thomas et al., 2016). The standardised breakfast, prior to the exercise tests on Day 0, was ingested 2 h preceding the tests (1.3 ml water, 0.9 g CHO, 0.3 g protein, 0.2 g fat and 0.1 g dietary fibre kg⁻¹ BM, respectively). The diets consisted mainly of oatmeal, milk, wheat flour bun, rye bread, chicken, pasta and yoghurt.

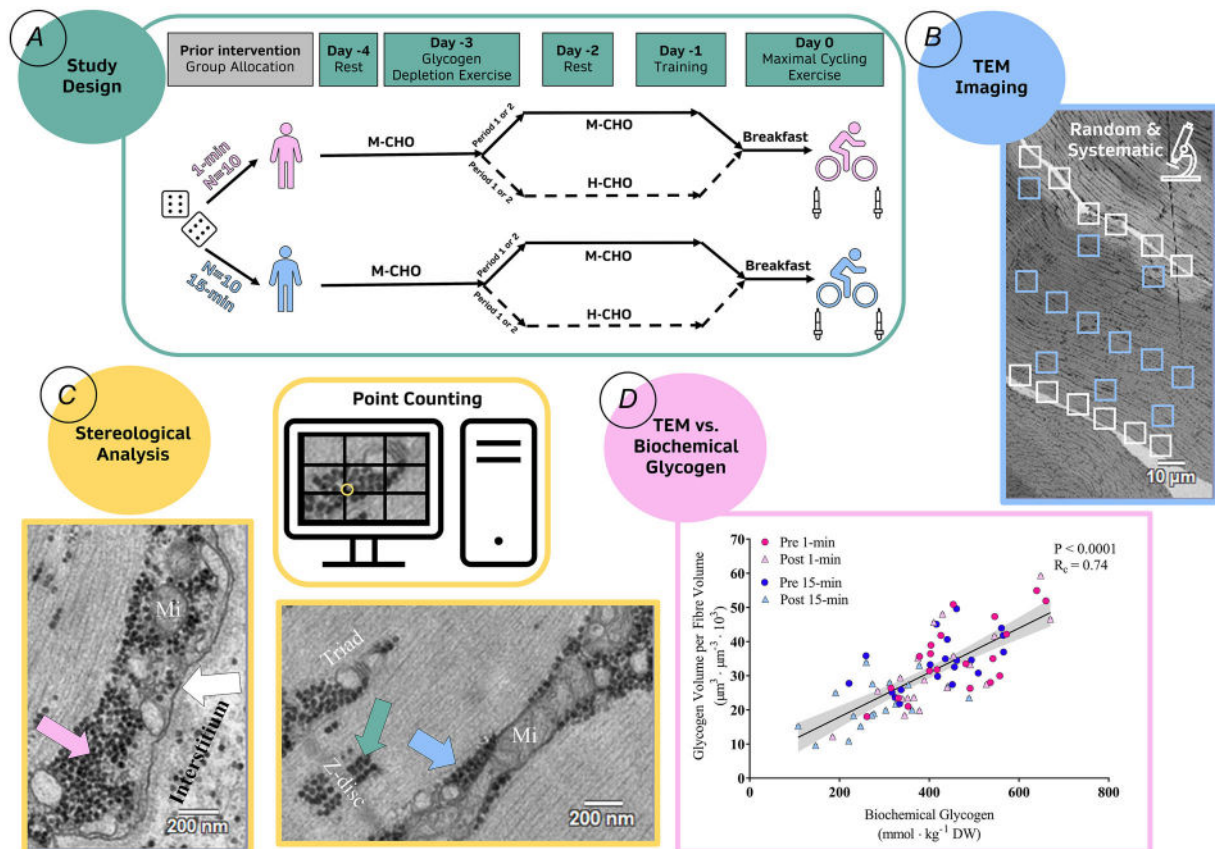


Figure 1. Study design and methods

A, the participants were randomised to perform two maximal cycling exercise tests of either 1 min ($n = 10$) or 15 min ($n = 10$) at the end of two dietary intervention periods consisting of either a moderate (M-CHO) or high (H-CHO) amount of CHO and energy following glycogen-depleting exercise. The participants repeated this after a 10-day period (in a randomised order), where they ingested the opposite diet. Muscle biopsies from the *m. vastus lateralis* were extracted pre and post each exercise test. B, each longitudinally oriented fibre was photographed by a transmission electron microscope in a random but systematic order including 12 images from the subsarcolemmal region (white boxes), and 12 images from the myofibrillar region (blue boxes). C, glycogen volume density and particle diameter were estimated in the intermyofibrillar (blue arrow), intramyofibrillar (green arrow) and subsarcolemmal (pink arrow) localisations. Grids were overlaid each image for manual point counting (example shown with yellow circle). Sarcolemma indicated by white arrow. Example shown of a mitochondrion (Mi), Z-disc, and triad junction consisting of the arrangement of a transverse tubuli with an adjacent terminal cisterna of the sarcoplasmic reticulum on each side. D, TEM-estimated (and myosin heavy chain (MHC) weighted) glycogen content plotted against biochemical-determined glycogen content. Pre and post values are shown from the maximal cycling exercise of either 1 or 15 min with line of regression and corresponding 95% confidence interval (grey area). R_c : Lin's concordance correlation coefficient based on values normalised to the mean.

The excess carbohydrates in the H-CHO diet were wine gums and diluted blackcurrant concentrate. To balance the protein content between diets, protein powder was added to the M-CHO diet. The physical activity level was strictly controlled during the intervention periods, and day-to-day diaries confirmed that the participants adhered to these restrictions.

Preliminary tests

Preliminary tests were conducted ~1 to 2 weeks before the first training day (Day -3). The participants were instructed to refrain from strenuous physical activity, alcohol, as well as tea and coffee from 18.00 h the day before. Upon arrival at the laboratory, their height and weight (Tanita MC-780MA, Frederiksberg, Denmark) were determined. Then they performed an incremental test to exhaustion to determine $\dot{V}_{O_{2,max}}$ and maximal power output ($PO_{max,incremental}$), followed by familiarisation to the glycogen depleting protocol and training session (i.e. on Day -3 and -1, respectively). Finally, the participants completed a familiarisation trial of either the 1-min or 15-min maximal exercise test depending on their random allocation.

The incremental test was performed using a pre-calibrated electromagnetic cycling ergometer (Schoberer Rad Messtechnik (SRM), Jülich, Germany) where settings were individualised, and the participants used similar shoes and settings during the glycogen-depleting exercises, training sessions and exercise tests. The incremental test was conducted in a seated position and commenced with a load of 100 W and increased by 25 W every third minute until voluntary exhaustion. A Quark CPET mixing chamber system (Cardio Pulmonary Exercise Test) (COSMED, Albano Laziale, Italy) was used to analyse expired \dot{V}_{O_2} and \dot{V}_{CO_2} in 10-s intervals during the incremental test (and the 1- and 15-min tests). Prior to each test, gas analysers were calibrated with known O_2 and CO_2 concentrations, and the flow meter calibrated manually with a 3-litre syringe. Moreover, the laboratory was continuously ventilated to maintain constant temperature and composition of the ambient air. $\dot{V}_{O_{2,max}}$ was defined as the highest 30 s average of three consecutive 10 s \dot{V}_{O_2} measurements. $PO_{max,incremental}$ was determined as the power output of the last completed step plus 25 W times the fraction completed of the last step before reaching $\dot{V}_{O_{2,max}}$.

Glycogen-depleting exercise and training session

On Day -3 (Fig. 1A), the participants performed the glycogen depletion exercise protocol consisting of both ergometer cycling (on a pre-calibrated SRM ergometer) and arm cranking. The protocol is described in a

companion paper (Schytz et al. 2023). Arm exercise was incorporated to reduce glycogen levels in a significant portion of the total muscle mass. This was done to investigate the relationship between glycogen content, body mass and cycling performance in a companion study (Schytz et al., 2023). Overall, the participants performed a mix of short-term all-out efforts and prolonged continuous exercises. Hereafter, they were randomised in a counterbalanced order to receive either the M-CHO or H-CHO diet. The training session on Day -1 consisted of a 10-min warm-up at 100 W and 4×2 min at 100% of $PO_{max,incremental}$ separated by 2 min of rest on an air- and magnetic-braked cycling ergometer (Wattbike Pro, Wattbike Ltd, Nottingham, UK).

Maximal cycling exercise of 1 min and 15 min

At test days (Day 0), the participants performed one of the two maximal cycling exercise tests (1 min or 15 min) on the pre-calibrated SRM cycling ergometer. Since high-intensity exercise as part of the warm-up procedure has been shown to improve subsequent exercise performance (Bishop et al., 2003), a pre-warmup consisting of 5 min at 100 W followed by 3×1 min at 100% of $PO_{max,incremental}$, each separated by 1 min of rest, was conducted 30 min before the exercise tests. After the warm-up a muscle biopsy was extracted before the participants warmed up for another 5 min at 100 W. After a short break, the participants increased the cadence to 60 rpm (at a low power output, i.e. <70 W), and the 1- and 15-min tests were then initiated following a 3-s countdown. Cadence was fixed at 110 rpm and 90 rpm in the 1- and 15-min maximal cycling exercise, respectively. During the 1-min test, power output was not visible for the participants, time was announced orally every 10th second, and the test ended with a 5-s countdown. Prior to the 15-min test, participants were provided with a recommended starting load of 90% of $PO_{max,incremental}$ and were allowed to monitor power output on an adjacent monitor during the first minute of the test. Thereafter, power output was concealed, and time was announced orally every minute during the first 11 min, every 30 s for the following 3 min and every 10th second during the last minute, ending with a 5-s countdown. Verbal encouragement was standardised in both tests (i.e. same phrase and tone of voice, given at the same time points). Participants remained seated throughout the test and were instructed to generate the highest possible average power output during the test. The mean power output across diets was (mean [95% confidence interval]) 572 W [519, 625] and 293 W [264, 323] during the 1-min and 15-min maximal cycling exercise tests, corresponding to 188% [181, 195] and 94% [91, 98] of $PO_{max,incremental}$, respectively. Technical issues leading to wrong cadence

caused the exclusion of one 1-min test in the H-CHO condition. A muscle biopsy was extracted immediately after the exercise tests. Average power output during the tests and perceived exertion rated immediately after the tests have been reported previously in Schytz et al. (2023). Moreover, \dot{V}_{O_2} was measured continuously during the test and used to estimate anaerobic energy contribution (see details below).

Determination of anaerobic contribution and glycogen utilisation per external work

The anaerobic energy contribution was calculated based on estimates of the accumulated oxygen deficit (Medbø et al., 1988). First, the individual power– \dot{V}_{O_2} relationship was established based on an average of \dot{V}_{O_2} in the last 60 s of each of the 6–12 submaximal steps of the incremental test. This relationship was used to estimate the \dot{V}_{O_2} needed to cover the energy demand during the 1- and 15-min maximal cycling exercise tests obtained in 10-s intervals by measurements of power output. The accumulated oxygen deficit for each maximal cycling exercise test was then estimated as the sum of the differences between the calculated O_2 demand and the measured O_2 consumption in each 10-s interval. The maximal cycling exercise tests and the incremental test were performed under the same conditions with respect to diet and fluid intake to ensure that differences in the measured \dot{V}_{O_2} was not affected by dietary differences.

The anaerobic energy contribution during the 1- and 15-min maximal cycling exercise was estimated to be on average 64.6% and 4.5% of total energy turnover, respectively (Schytz et al., 2023). Knowing the relative contributions of energy from aerobic and anaerobic sources enabled a calculation of the ATP yield per glycosyl unit during the 1- and 15-min test assuming a yield of 3 and 36 ATP per glycosyl unit during anaerobic and aerobic conditions, respectively (Hargreaves & Spriet, 2018): 1 min: $(36 \times 0.354 + 3 \times 0.646) = 14.7$ ATP per glycosyl unit, and 15 min: $(36 \times 0.955 + 3 \times 0.045) = 34.5$ ATP per glycosyl unit, giving a ratio (1 min/15 min) of 0.43. Thus, due to the larger aerobic contribution during the 15-min maximal exercise and consequently a higher ATP yield per glycosyl unit, a 0.43 times lower amount of glycogen utilisation per external work is expected during the 15-min maximal exercise than during the 1-min maximal exercise. The actual utilisation of the three pools of glycogen (see method below) per amount of external work was calculated as the pre minus the post glycogen value and then divided by the external work performed (i.e. average power output per kg BM times the duration (s)). The values within each maximal exercise for each subcellular region were averaged, and to compare the expected and actual utilisation per external work during

the 15-min maximal exercise, the averaged values from the 1-min maximal exercise was multiplied by 0.43, which is indicated by the dashed lines in Fig. 3. This helps determine whether the glycogen utilisation rate is sensitive to the differential contributions from the aerobic and anaerobic metabolism for the specific glycogen pools.

Muscle biopsy extraction and handling

Muscle biopsies were extracted from the m. vastus lateralis before and immediately after (1–2 min) each 1- and 15-min test using the Bergström needle technique with suction through incisions made with scalpels under local anaesthesia (2% lidocaine). The incision for the biopsy extracted immediately after the test was made prior to the test. For each exercise test the pre and post biopsies were extracted from the same leg, changing to the contralateral leg in the next test (i.e. H-CHO or M-CHO condition), with the leg randomly chosen and left and right leg equally distributed for each diet. The extracted muscle tissue was placed on filter paper on an ice-cooled Petri dish, blotted dry, and visible connective tissue and fat removed. The muscle tissue was divided into three specimens used in this study. The first specimen was snap frozen in liquid nitrogen and stored at -80°C until biochemical determination of glycogen content. The second specimen was homogenised, frozen in liquid nitrogen and stored at -80°C for determination of myosin heavy chain (MHC) composition. The third specimen ($\sim 1 \text{ mm}^3$) was immediately fixed with 2.5% glutaraldehyde in 0.1 M sodium cacodylate buffer (pH 7.3) for 24 h at 5°C , then rinsed 4×15 min in 0.1 M sodium cacodylate buffer and stored in 0.1 M sodium cacodylate buffer at 5°C until further processing for TEM. Two post test biopsies in the 15-min group were not analysed due to technical errors in the tissue preparation phase.

Biochemical determination of glycogen

Muscle glycogen content was determined spectrophotometrically (Beckman DU 650, Beckman Instruments, Fullerton, CA, USA) as previously described in detail in Gejl et al. (2014).

MHC composition

MHC composition was determined as previously described in Schytz et al. (2023), and was, in brief, determined in homogenate (made with a Potter-Elvehjem glass–glass homogenizer (Kontes Glass Industry, Vineland, NJ, USA) from two biopsies (left and right leg) using SDS-PAGE where the MHC bands were made visible using Coomassie staining. The values are reported in a companion paper (Schytz et al., 2023) and included

in this paper to weigh TEM-estimated glycogen measures according to individual MHC composition to be able to compare these values with biochemically determined glycogen content (see below).

Preparation of muscle specimen for transmission electron microscopy

Muscle specimens were prepared as described by Jensen et al. (2022). In brief, muscle specimens were post-fixed with 1% osmium tetroxide and 1.5% potassium ferrocyanide in 0.1 M sodium cacodylate buffer for 120 min at 4°C. Afterwards the muscle specimens were rinsed two times in 0.1 M sodium cacodylate buffer at room temperature, dehydrated through graded series of alcohol at room temperature, infiltrated with graded mixtures of propylene oxide and Epon at room temperature, and embedded in 100% fresh Epon in moulds and polymerized at 60°C for 48 h. The blocks of embedded fibres were cut in sections of longitudinally oriented fibres using a Ultracut UCT ultramicrotome (Leica Microsystems, Wetzlar, Germany) in ultra-thin sections (~60 nm). These sections were contrasted with uranyl acetate and lead citrate, and later examined by TEM.

Imaging of muscle fibres by transmission electron microscopy

The sections were photographed by the same blinded investigator in a pre-calibrated EM 208 transmission electron microscope (Philips, Eindhoven, The Netherlands) with a Megaview III FW camera (Olympus Soft Imaging Solutions, Münster, Germany). From each section (biopsy) 8–10 longitudinal oriented fibres were imaged at $\times 13,500$ magnification in a randomised but systematic and uniform order (Fig. 1B). From each fibre, 24 images were obtained, including 12 images from the subsarcolemmal region and 12 images from the myofibrillar region of which six images were from both the superficial and central parts (Fig. 1B).

Z-disc-based single fibre analyses

To investigate associations between fibre types and utilisation of the subcellular glycogen pools, the average Z-disc thickness of each fibre was estimated based on 12 random locations (one per myofibrillar image). To ensure that both fibre types are represented, the three fibres demonstrating the thickest and the three the thinnest Z-disc were included, leading to an exclusion of two to four fibres from each biopsy with intermediate Z-disc widths. The rationale for using Z-disc widths as an indicator for fibre type is based on work showing

that myofibrillar ATPase properties are associated with Z-disc widths (Sjöström, Ångquist, et al., 1982; Sjöström, Kidman, et al., 1982). The analysis was accomplished by the same blinded investigator.

Quantification of subcellular glycogen volume densities

Glycogen was quantified in three subcellular localisations within the muscle fibre: (1) the intermyofibrillar space, (2) the intramyofibrillar space, and (3) the subsarcolemmal space (Fig. 1C) (Jensen et al., 2022). The glycogen volume fraction (V_V), taking the effect of section thickness into account, was estimated as proposed by Weibel (1980), assuming that glycogen particles are spherical (Melendez-Hevia et al., 1993): $V_V = A_A - t \left((1/\pi) B_A - N_A [(t \times H)/(t + H)] \right)$, where A_A is glycogen area density (see estimation below), t is the section thickness (i.e. 60 nm), and H is the mean glycogen particle profile diameter assessed by direct measurement (see below). N_A is the number of particles per area determined by dividing the estimated area density (A_A) by the average glycogen particle area calculated by assuming a circular profile of the glycogen particles and employing the measured mean particle diameter. The glycogen boundary length density is given by: $B_A = (\pi/4) S_V + t N_V \pi H$. Here, the surface area density (S_V) can be estimated as: $S_V = N_V s$ where s is the mean particle surface area estimated by assuming a spherical particle and the numerical volume density (N_V) is given by, $N_V = N_A/(tH)$ (Weibel, 1980).

The glycogen area fraction was estimated by point counting since $A_A = P_P$, where P_P is the glycogen point density (Weibel, 1980). The intermyofibrillar glycogen content was expressed relative to the myofibrillar space, which mainly consists of the myofibrils, mitochondria, sarcoplasmic reticulum (SR), t-system, glycogen and lipids. The intramyofibrillar glycogen content was expressed relative to the intramyofibrillar space consisting solely of the myofibrils. Glycogen estimates localised in the superficial region of the myofibrillar space were weighted three times higher than those in the central region since this region takes up 75% of the fibre volume when muscle fibres are assumed to be cylindrically shaped.

The subsarcolemmal region is defined as the region between the sarcolemma and the outermost myofibril consisting mainly of mitochondria, nuclei, glycogen and lipids. To avoid a bias induced by changes in these parameters during the maximal cycling exercise tests, the subsarcolemmal glycogen was expressed relative to the muscle fibre surface area, as estimated from length measurement of the outermost myofibril running parallel with the fibre surface membrane multiplied by the section thickness (i.e. 60 nm).

The total glycogen volume per fibre volume is the sum of all three pools and is used to estimate the relative distribution of the pools. Since the subsarcolemmal glycogen is expressed as volume per myofiber surface area, it was converted to volume per fibre volume. This was obtained by dividing the raw data by 20, since assuming cylindrical fibres, the volume, V , beneath a surface area of $1 \mu\text{m}^2$ is $20 \mu\text{m}^3$. This can be realised by first calculating the surface area, A , of this 'slice' given by $A = 0.5 \times r \times 1 \mu\text{m}$, where r is the fibre radius assumed to be $40 \mu\text{m}$. Then to obtain the volume, this surface area is multiplied by the depth of the 'slice' (i.e. $1 \mu\text{m}$). Thus, $V = 0.5 \times 40 \mu\text{m} \times 1 \mu\text{m} \times 1 \mu\text{m} = 20 \mu\text{m}^3$. Also, the intramyofibrillar glycogen volume per intramyofibrillar volume was re-calculated to per fibre volume. This was conducted by multiplying the original value with the intramyofibrillar to myofibrillar volume ratio.

Grids were overlaid each image for point counting, and different sizes were applied based on expected area fractions to balance the workload of the analysis and the coefficient of error. Thus, grid sizes used for point counting were $400 \times 400 \text{ nm}$, $173 \times 173 \text{ nm}$, $63 \times 63 \text{ nm}$ for the intramyofibrillar space, intermyofibrillar glycogen and intramyofibrillar glycogen, respectively, in a frame size of $3.4 \mu\text{m}$ wide and $2.43 \mu\text{m}$ long. The grid size was $316 \times 316 \text{ nm}$ for subsarcolemmal glycogen. The coefficient of error (CE_{est}) values, estimated as proposed for stereological ratio estimates by Howard and Reed (2005), were 0.12, 0.14, and 0.20 for intermyofibrillar, intramyofibrillar, and subsarcolemmal glycogen, respectively. The mean particle diameter was assessed by measuring the diameter of a minimum of 60 particles per fibre per subcellular localisation (Jensen et al., 2022). Only particles with distinct diameter (i.e. non-overlapping) were included, and to avoid selection bias included particles were randomly chosen. The average particle volume (size) was estimated by assuming a spherical structure (Melendez-Hevia et al., 1993) and employing the average particle diameter for each measurement, while numerical particle density was calculated by dividing the estimated glycogen volume densities by the average particle volume.

Glycogen quantification was performed by four trained investigators where all fibres from a participant were analysed by the same investigator. Inter-investigator analyses of 24–35 randomly chosen images showed a bias up to 23% and a coefficient of variation of up to 7% evaluated as proposed by Bland and Altman (1986). The raw data were adjusted for the biases. Also, particle diameters were adjusted for biases of up to 17%. All measurements were blinded and performed in ImageJ (ImageJ 1.53e, National Institutes of Health, Bethesda, MD, USA).

To validate TEM-estimated glycogen against biochemically determined glycogen, total glycogen

volume densities of type 1 and 2 single fibres (based on Z-disc width) were averaged for each participant according to diet, time point and test. The average type 1 and 2 fibre values were weighted according to individual MHC composition enabling calculation of MHC-weighted TEM-estimated total glycogen volume densities. These values were for each time point and test plotted against the corresponding biochemically determined glycogen content (Fig. 1D). Including all time points for both tests, a substantial concordance was found ($R_c = 0.74$) (Fig. 1D), and moderate to substantial concordances were found within time points for each test ($R_c = 0.53$ – 0.74).

Statistics

Linear mixed models were applied in all analyses because of the repeated measures design, multiple fibres from each biopsy and missing values. Thus, descriptive parameters (i.e. age, body mass, height, $\dot{V}_{\text{O}_2\text{max}}$ and $\text{PO}_{\text{max,incremental}}$) were compared between participants completing either the 1- or 15-min of maximal exercise by including the exercise test as a fixed effect (Table 1). Further, to analyse the effect of exercise test (1 or 15 min) on subcellular glycogen content and relative contribution of each pool to total glycogen, time, test, and time \times test interaction were included in the model as fixed effects and participant and time as random effects (Fig. 2). How exercise test affected glycogen utilisation per external work was analysed with test as fixed effect (Fig. 3). The effect of lowering dietary carbohydrates and energy content prior to the 1- and 15-min tests (Fig. 6) was examined with diet as fixed effect and participant and fibre type as random effects. The effects of each exercise test (Figs 7 and 8) on subcellular glycogen content, relative contribution of each pool to total glycogen, glycogen particle volume and numerical density were examined with time, diet, and time \times diet interaction as fixed effects and participant and time as random effects. All main effects and interactions were tested by a Wald test and if significant, pairwise comparisons were conducted.

Linear mixed models were validated by examining model assumptions: normal distribution of standardised residuals were investigated by visual inspection of Q–Q plots, and by the Shapiro–Wilks test and a skewness and kurtosis test for normality. Moreover, variance homoscedasticity was investigated by visual inspection of standardised residuals plotted against the predicted values and by running a Breusch–Pagan/Cook–Weisberg test for heteroskedasticity on a linear regression model including all fixed effects for the respective model. If model assumptions were violated data were transformed.

Lin's concordance correlation coefficient (R_c) was calculated to validate MHC-weighted total

TEM-estimated glycogen against biochemically determined glycogen by testing the agreement with the line of identity, where R_c is defined on a scale where 0.21–0.40 is fair, 0.41–0.60 is moderate, 0.61–0.80 is substantial and 0.81–1.00 is almost perfect concordance (Lin, 1989). This analysis was performed with individual participant values relative to the mean (Fig. 1D). Correlation analysis between glycogen content in all subcellular regions and Z-disc width were analysed in each exercise test separately and were performed using Pearson's correlation coefficient. The best fit is stated for each correlation evaluated by the strength of the coefficient of determination (R^2) evaluated on a scale with <0.20 as weak, 0.21–0.40 as fair, 0.41–0.60 as moderate, 0.61–0.80 as good and 0.81–1.00 as a very good strength (Fig. 5).

All values are presented as median (interquartile range) unless stated otherwise. Number of participants included in the analysis was 10 in each exercise test. In all statistical tests a significance level of $\alpha < 0.05$ was used. Stata/BE

17.0 (StataCorp, College Station, TX, USA) was used to conduct the statistical analysis, while figures were constructed in GraphPad Prism 7.05 (GraphPad Software, La Jolla, CA, USA).

Results

Utilisation of the subcellular glycogen pools during 1- and 15-min maximal cycling exercise and the relation to the performed external work

In a companion paper we found that 34 [−62, −5] and 138 [−168, −108] mmol kg^{−1} dry weight (DW) (mean [95% confidence interval]) of glycogen was utilised across diets during 1- and 15-min maximal exercise, respectively (Schytz et al., 2023). This exercise-induced reduction of whole-muscle glycogen, determined biochemically, was then expanded on using TEM, investigating if the three distinct subcellular pools of glycogen were affected differently by the two exercise tests across diets.

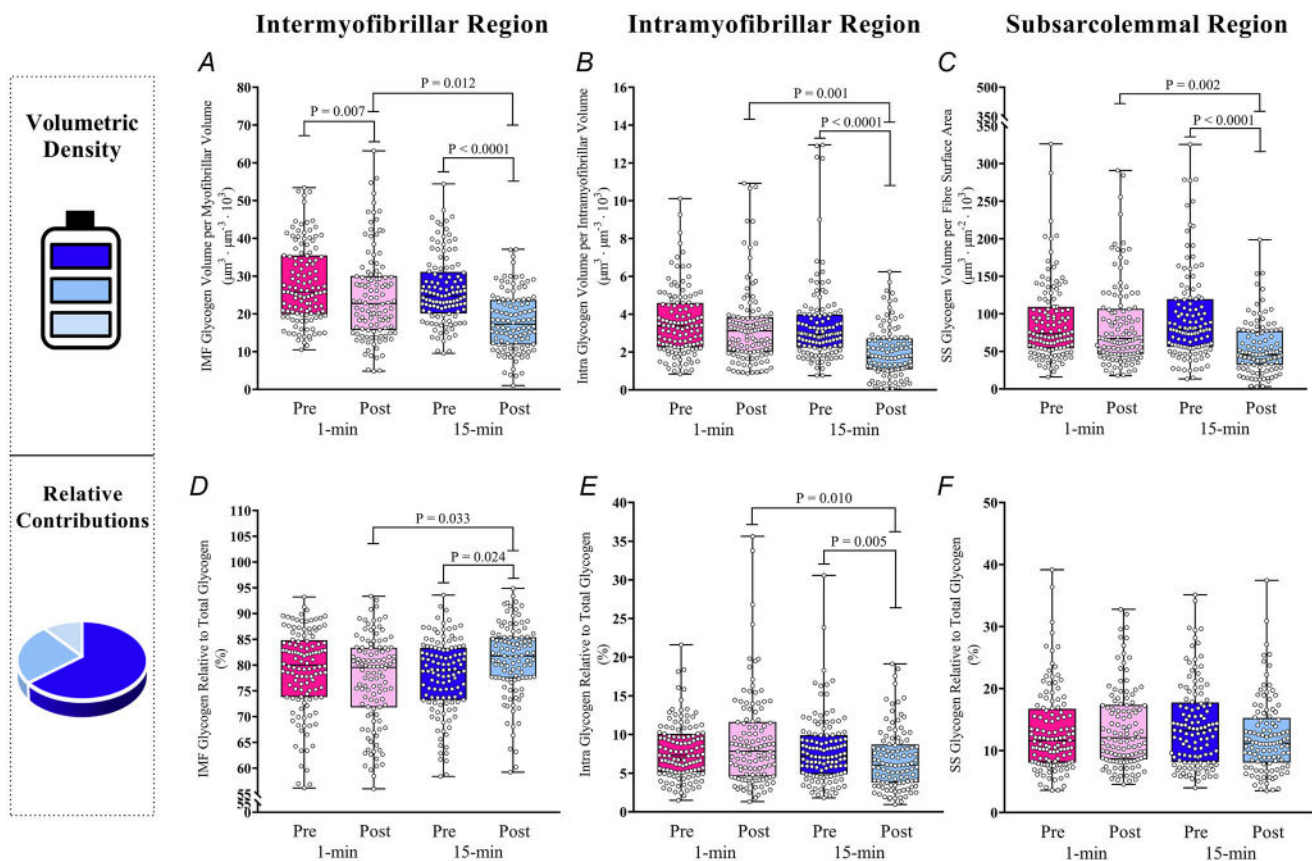


Figure 2. Differential spatial utilisation of muscle glycogen during 1-min versus 15-min maximal cycling exercise

Values are from biopsies obtained before (pre) and immediately after (post) 1-min and 15-min maximal cycling exercise. A–C, glycogen volumetric density; D–F, relative contribution to total glycogen. Data shown as median (interquartile range). All individual fibres are displayed as a circle with 6 fibres from each participant. 1-min Pre: $n = 120$, Post: $n = 114$, and 15-min Pre: $n = 120$, Post: $n = 108$. P -values represent pairwise comparisons from linear mixed model. IMF, intermyofibrillar; Intra, intramyofibrillar; SS, subsarcolemmal.

After the 1-min maximal exercise, the largest reduction was observed in the intermyofibrillar pool of glycogen ($\sim 12\%$), compared to the intramyofibrillar and subsarcolemmal pools of glycogen ($\sim 8\%$ – 9% ; Fig. 2A–C). In contrast, after the 15-min maximal exercise, the largest reductions were observed in the intramyofibrillar and subsarcolemmal pools ($\sim 41\%$ – 43%), as compared to the intermyofibrillar pool of glycogen ($\sim 30\%$; Fig. 2A–C). Thus, the two exercise tests had differential effects on the distinct subcellular pools of glycogen. This was also clear if glycogen was expressed as a relative distribution, where the share of intermyofibrillar glycogen increased after the 15-min maximal exercise (time \times test: $P = 0.008$; Fig. 2D) and intramyofibrillar decreased after the 15-min maximal exercise (time \times test: $P = 0.008$; Fig. 2E).

The contribution from anaerobic metabolism to the performed external work was estimated (Medbø et al., 1988; see Methods) to be 64.6% on average during the 1-min maximal exercise and 4.5% during the 15-min maximal exercise (Schytz et al., 2023). With a 12-fold higher ATP yield per glycosyl units by aerobic metabolism than anaerobic metabolism, the glycogen utilisation per external work was expected to be 0.43 times lower during the 15-min maximal exercise than during the 1-min maximal exercise (see Methods). The utilisation of intermyofibrillar glycogen per external work was indeed less than half during the 15-min maximal cycling exercise compared to the 1-min maximal cycling exercise, while the utilisation of both intramyofibrillar and sub-

sarcolemmal glycogen per external work was not different between the 1- and 15-min maximal exercise tests (Fig. 3).

Single fibre glycogen pools

Fibre-to-fibre variability in the three pools of glycogen (Fig. 4) revealed a higher variability (coefficient of variation) in the volumetric density of intramyofibrillar (0.63) and subsarcolemmal (0.66) glycogen than of intermyofibrillar glycogen (0.43). Single fibre analyses also suggested that the utilisation of glycogen was remarkably homogeneous across fibres in all subcellular pools during 1- and 15-min maximal cycling exercise (Fig. 4). Sorting the single fibres based on the Z-disc width enables a discrimination between fibre types, with type 1 fibres having a relatively wider Z-disc than type 2 fibres. Prior to both the 1- and 15-min test, a weak negative correlation was found between the Z-disc widths and intermyofibrillar glycogen content suggesting higher pre-exercise glycogen levels in the type 2 fibres, while negligible fibre type differences were observed in the pre-exercise intramyofibrillar and subsarcolemmal glycogen content (Fig. 5A–F). After both the 1- and 15-min maximal cycling exercise, the drop in intermyofibrillar and intramyofibrillar glycogen volume densities was slightly more pronounced in fibres with a thin Z-disc than in fibres with a thick Z-disc suggesting a slightly larger glycogen utilisation in type 2 fibres than in type 1 fibres (Fig. 5A, B, D, and E). This was not observed in the subsarcolemmal region (Fig. 5C and F).

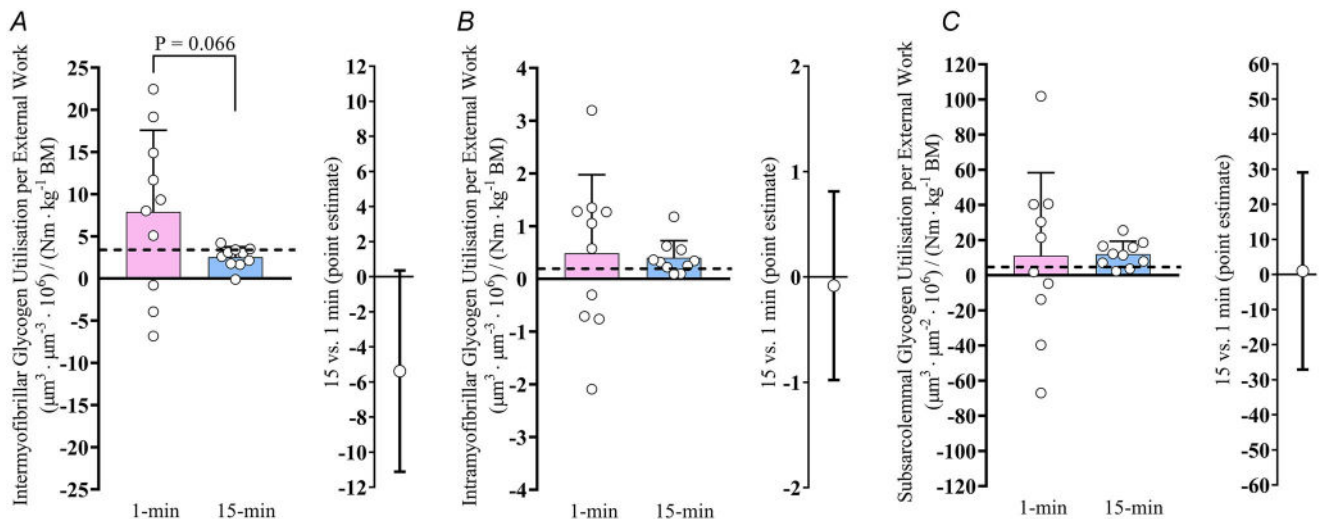


Figure 3. Glycogen utilisation rate per external work in the three subcellular pools of glycogen during the two different maximal cycling exercises

Glycogen utilisation per external work during 1-min and 15-min maximal cycling exercise in the three subcellular pools: intermyofibrillar (A), intramyofibrillar (B), and subsarcolemmal (C). The difference between the 1- and 15-min maximal exercise tests are shown as point estimates with corresponding 95% confidence intervals. The black dotted line represents the expected glycogen utilisation per external work during the 15-min maximal exercise (see Methods for details). Data are presented as mean (standard deviation), and the value for each participant is displayed as a circle. P -value represents the main effect of test from linear mixed model.

Effect of lowering carbohydrate and energy intake after glycogen-depleting exercise on pre-exercise glycogen pools, particle size and numerical density

Lowering the amount of dietary carbohydrates (from 10 to 4 g kg⁻¹ BM day⁻¹) equivalent to lowering the total energy intake (from 240 to 138 kJ kg⁻¹ BM day⁻¹) in M-CHO after the glycogen-depleting exercise, resulted in a 31% lower glycogen content than in H-CHO (mean [95% confidence interval]: 360 [329, 391] vs. 520 [489, 551] mmol kg⁻¹ DW, respectively) as presented in a companion paper (Schyetz et al., 2023). The TEM-based analysis of the subcellular glycogen distribution revealed that this diet-induced reduction in glycogen content was most pronounced in the intramyofibrillar and subsarcolemmal pools (Fig. 6A–C), as their relative contribution to total glycogen decreased as opposed to an increase in the contribution of intermyofibrillar glycogen (Fig. 6D–F). The direct measurement of glycogen particle size showed markedly smaller glycogen particles in all subcellular pools in M-CHO compared with H-CHO (Fig. 6G–I), and, to a lesser extent, fewer glycogen particles per volume in the intramyofibrillar (Fig. 6K) and subsarcolemmal (Fig. 6L) localisations, but not in the intermyofibrillar localisation (Fig. 6J). This unchanged numerical density of intermyofibrillar glycogen particles contributed to a lower diet-induced reduction of glycogen content in this specific localisation, and consequently that inter-

myofibrillar glycogen constituted a greater part of total glycogen content in M-CHO than H-CHO (Fig. 6D–F).

Thus, the lower CHO and energy intake following glycogen-depleting exercise (combined with controlled training session on Day –1) resulted in smaller glycogen particles and localisation-specific fewer particles per volume, with a lower numerical particle density in the intramyofibrillar and subsarcolemmal localisations.

Effects of 1- or 15-min maximal cycling exercise in the M- or H-CHO conditions on glycogen pools, particle size and numerical density

We next examined how this altered storage (size, numerical density and localisation) of glycogen was associated with the utilisation of glycogen during 1- and 15-min maximal cycling exercise. After the 1-min maximal exercise, the volumetric density of intermyofibrillar glycogen was reduced by ~25% in M-CHO, but unchanged in H-CHO (time × diet: $P = 0.008$) (Fig. 7A). Intramyofibrillar and subsarcolemmal glycogen were either unchanged or reduced by up to ~10%–20%, irrespective of diet (time × diet: $P = 0.337$ and $P = 0.748$; main effect time: $P = 0.137$ and $P = 0.219$, respectively) (Fig. 7B and C). If the three pools are expressed as a relative distribution of total glycogen content, only minor alterations were observed between M-CHO and

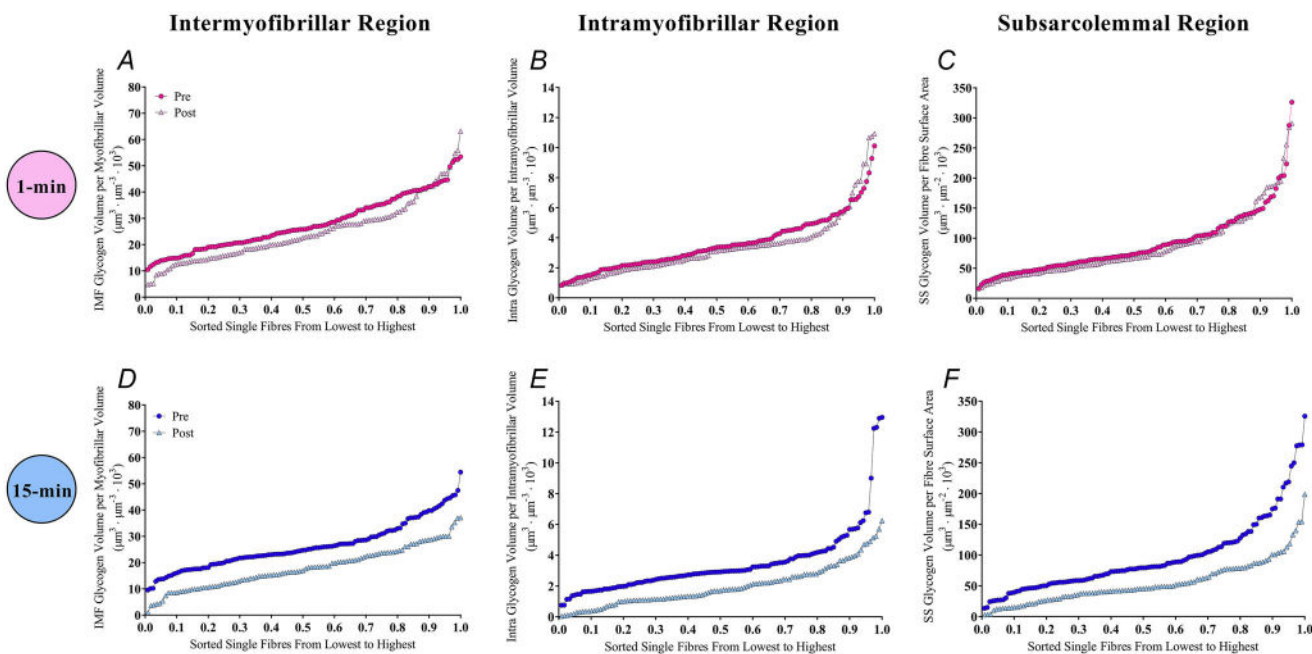


Figure 4. Single fibre glycogen values revealed a fibre-to-fibre homogeneous lowering of glycogen during maximal exercise

Glycogen content of single fibres at pre and post 1-min (A–C) and 15-min (D–F) maximal cycling exercise from the intermyofibrillar, intramyofibrillar and subsarcolemmal region. Fibres are ordered in relation to glycogen content and weighed according to the number of fibres. 1-min Pre: $n = 120$, Post: $n = 114$, and 15-min Pre: $n = 120$, Post: $n = 108$. IMF, intermyofibrillar; Intra, intramyofibrillar; SS, subsarcolemmal.

H-CHO (time \times diet: Intermyoibrillar: $P = 0.055$, intramyofibrillar: $P = 0.455$, and subsarcolemmal: $P = 0.035$) (Fig. 7D–F).

To further understand how the glycogen pools were regulated during 1-min maximal cycling exercise in the M- and H-CHO conditions, we investigated the effect on glycogen particle size and numerical density. Interestingly, the reduction in the volumetric density of intermyofibrillar glycogen in M-CHO was primarily driven by a reduction in the numerical density (time \times diet: $P = 0.0006$) (Fig. 7J), with only a small change in the average particle size (time \times diet: $P = 0.505$; main effect time: $P = 0.018$) (Fig. 7G; and see Fig. 9A). The intramyofibrillar and subsarcolemmal glycogen particles did not, or only to a small extent, change in size or numerical density following the 1-min maximal cycling exercise, irrespective of diet (time \times diet: intramyofibrillar: $P = 0.108$ and 0.854 , respectively; subsarcolemmal: $P = 0.465$ and 0.878 , respectively) (Fig. 7H, I, K and L; and see Fig. 9B and C).

The 15 min of maximal cycling exercise mediated reductions in the volumetric density of glycogen in

all subcellular pools with no difference between diets (time \times diet: $P = 0.272$, $P = 0.401$, and $P = 0.727$, respectively) (Fig. 8A–C). The reductions were more pronounced in the intramyofibrillar and subsarcolemmal localisations than in the intermyofibrillar localisation, resulting in a decrease in the relative contribution of intramyofibrillar glycogen to total glycogen, and an increase in the relative contribution of intermyofibrillar glycogen to total glycogen irrespective of diet (time \times diet: $P = 0.240$ and $P = 0.786$, respectively) (Fig. 8D and E). The glycogen utilisation during the 15-min maximal exercise was explained by a decrease in both particle size and numerical density (Figs 8G–L and 9D–F).

Discussion

In human skeletal muscle fibres, glycogen is stored as discrete particles distributed heterogeneously throughout the fibre. In this study, we investigated how maximal exercise of two different intensities (1- and 15-min maximal cycling exercise) and lowered carbohydrate and

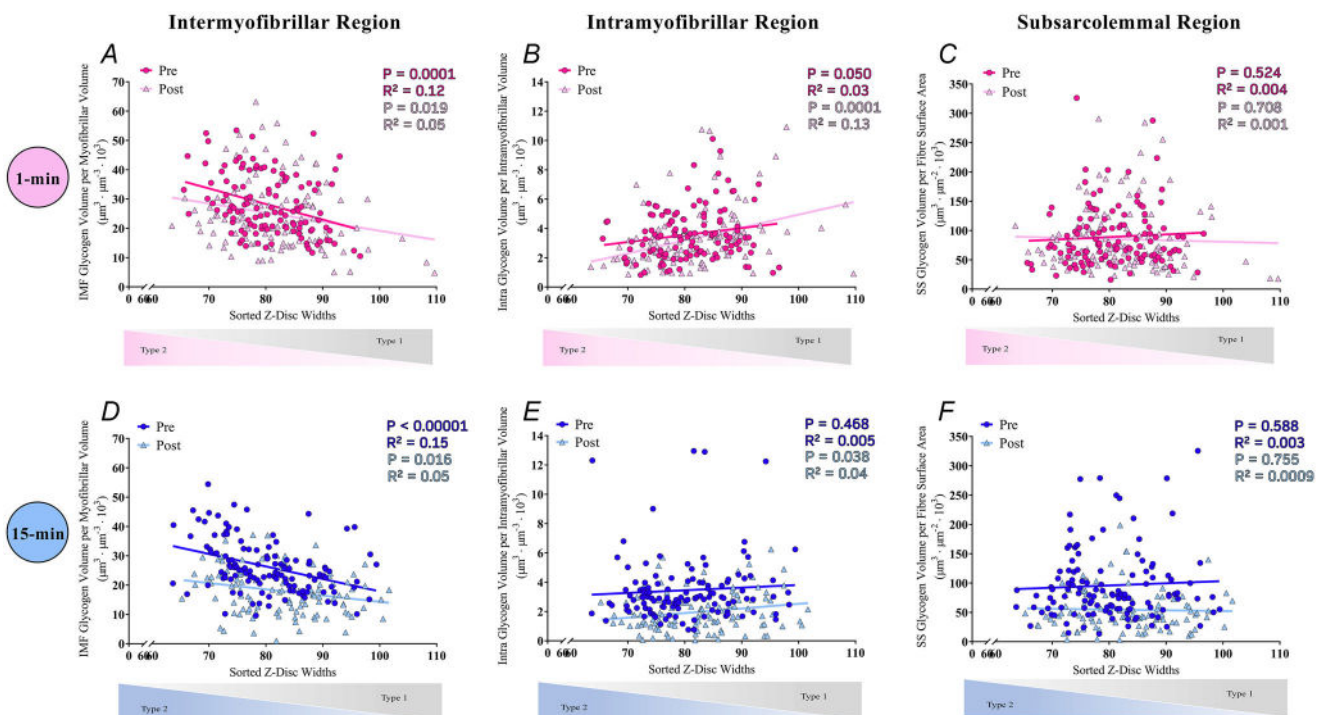


Figure 5. Single fibre Z-disc width suggests a slightly higher glycogen utilisation of type 2 fibres

Glycogen content of single fibres shown at pre and post 1-min (A–C) and 15-min (D–F) maximal cycling exercise from the intermyofibrillar (IMF), intramyofibrillar (Intra), and subsarcolemmal (SS) localisations, respectively. Type 1 fibres have broader Z-disc width (nm) than type 2 fibres (see Methods). Fibres are ordered in relation to glycogen content on the y-axis and Z-disc width on the x-axis. 1-min Pre: $n = 120$, Post: $n = 114$, and 15-min Pre: $n = 120$, Post: $n = 108$.

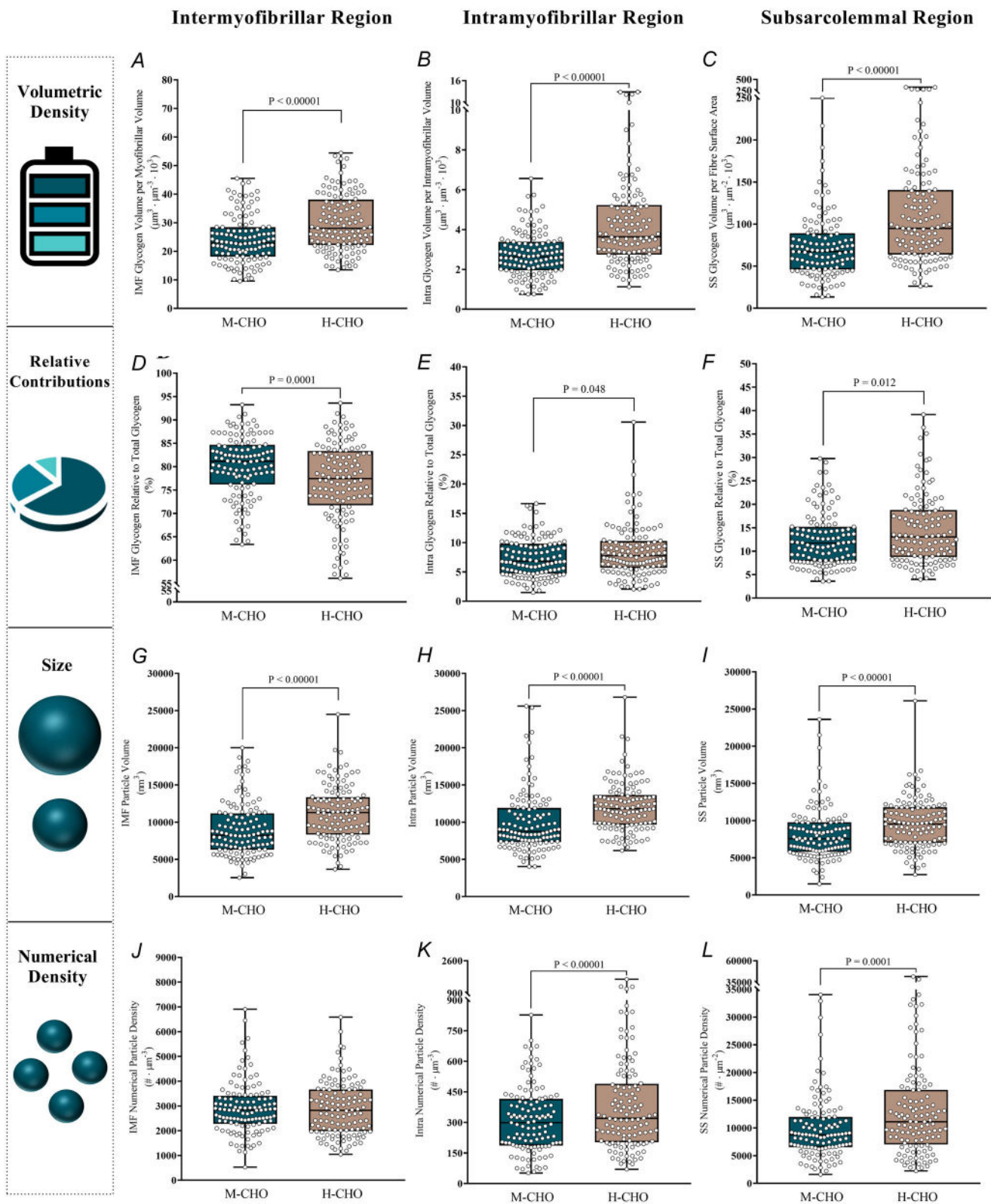


Figure 6. Lowering of the CHO and energy intake after glycogen-depleting exercise reduced the glycogen particle size

All values originate from the biopsies obtained before the exercise. A–C, glycogen volumetric density; D–F, relative contribution to total glycogen; G–I, particle size; J–L, numerical particle density. Data shown as median (inter-

quartile range). All individual fibres are displayed as a circle with six fibres from each participant. M-CHO: $n = 120$ and H-CHO: $n = 120$. P -values represent main effects from linear mixed model. IMF, intermyofibrillar; Intra, intramyofibrillar; SS, subsarcolemmal.

energy intake after glycogen-depleting exercise affected glycogen volume densities, particle size, numerical density and localisation within skeletal muscle fibres. The main findings of the study were that: (1) the two exercise tests were characterised by a differential utilisation of subcellular pools of glycogen, where intermyofibrillar glycogen was utilised relatively more than the other pools during 1 min of maximal cycling exercise, as opposed to a relative larger utilisation of intramyofibrillar glycogen during 15 min of maximal cycling exercise; (2) a lowered carbohydrate and energy intake after glycogen-depleting exercise decreased glycogen availability characterised by pronounced smaller glycogen particle sizes in all subcellular pools, and with fewer particles per volume within the intramyofibrillar and subsarcolemmal regions, but not in the intermyofibrillar region; (3) the observed glycogen utilisation during both of the two maximal cycling exercises was due to a decrease in both particle size and numerical density, and starting exercise with smaller particles was not associated with any effects on this pattern of glycogen utilisation.

Differential utilisation of subcellular pools during 1 and 15 min of maximal cycling exercise

During the 1 and 15 min of maximal cycling exercise, a differential utilisation of subcellular glycogen was observed, with a higher relative utilisation of intermyofibrillar glycogen during the 1-min test and a higher relative utilisation of intramyofibrillar glycogen during the 15-min test. The latter observation aligns with previous studies investigating glycogen utilisation during continuous exercise lasting 4–150 min (Gejl et al., 2017; Jensen, Ørtenblad, et al., 2020; Nielsen et al., 2011) or repeated high-intensity intermittent exercise (Vigh-Larsen et al., 2022). However, the former finding is, to the best of our knowledge, the first demonstration of this compartmentalised glycogen utilisation pattern in skeletal muscle during maximal exercise of such short duration. Furthermore, analyses of individual skeletal muscle fibres revealed consistently lower glycogen levels across all fibres compared with before the exercise test, and that type 2 fibres (as indicated by the Z-disc width) exhibited a slightly higher utilisation rate than type 1 fibres as expected during such high intensity exercise (Essén, 1978).

The differential utilisation of the three pools of glycogen between the two exercise tests (i.e. different intensities and durations) may be attributed to various factors. One of the key distinctions between the two maximal cycling

exercises is the contribution of anaerobic and aerobic metabolism to the ATP production. Here, we found that during the 1-min maximal exercise, there was a 64.6% contribution from anaerobic metabolism, while in the 15-min maximal exercise, this contribution was only 4.5% (Schytz et al., 2023). Given a 12-fold higher yield of ATP per glycosyl unit (glycogen) during aerobic processes than anaerobic processes (Hargreaves & Spriet, 2018), this difference has a substantial impact on the amount of glycogen required.

When comparing the expected and actual glycogen utilisation per external work during the 1 and 15 min of maximal exercise, we observed that the utilisation rates of the intramyofibrillar and subsarcolemmal pool of glycogen per external work performed were not different despite a large difference in the ratio of the energy contribution from aerobic and anaerobic processes. In contrast, the utilisation rate of intermyofibrillar glycogen per external work performed was less than half that during the 15-min maximal exercise, as expected given the higher aerobic contribution to this type of exercise. Consequently, intermyofibrillar glycogen is preserved during the 15 min of maximal exercise compared to the 1 min of maximal exercise. This preservation is likely due to the increased ATP yield from each glycosyl unit derived from intermyofibrillar glycogen during the aerobic processes. Thus, our findings suggest that during 15-min maximal exercise, metabolites originating from the degradation of intermyofibrillar glycogen can enter the mitochondria and undergo complete combustion. In contrast, metabolites generated through the breakdown of intramyofibrillar and subsarcolemmal glycogen cannot access the mitochondria. This speculation about compartmentalisation may arise from the proximity of intermyofibrillar glycogen to mitochondria, and the distant localisation of intramyofibrillar glycogen may prevent its interaction with mitochondria. However, subsarcolemmal glycogen particles are also found near mitochondria but showed contrary to the intermyofibrillar glycogen particles no sensitivity to the changes in the aerobic–anaerobic ratio between the 1- and 15-min tests. At present, the role of subsarcolemmal glycogen and mitochondria is unclear. The subsarcolemmal glycogen pool may provide energy for active transport mechanisms across the sarcolemma, which preferentially use glycolytically derived ATP (Dutka & Lamb, 2007; James et al., 1999; Jensen, Nielsen, et al., 2020). This could explain why this pool of glycogen was insensitive to changes in the anaerobic–aerobic conditions. It has been suggested, however, that energy can

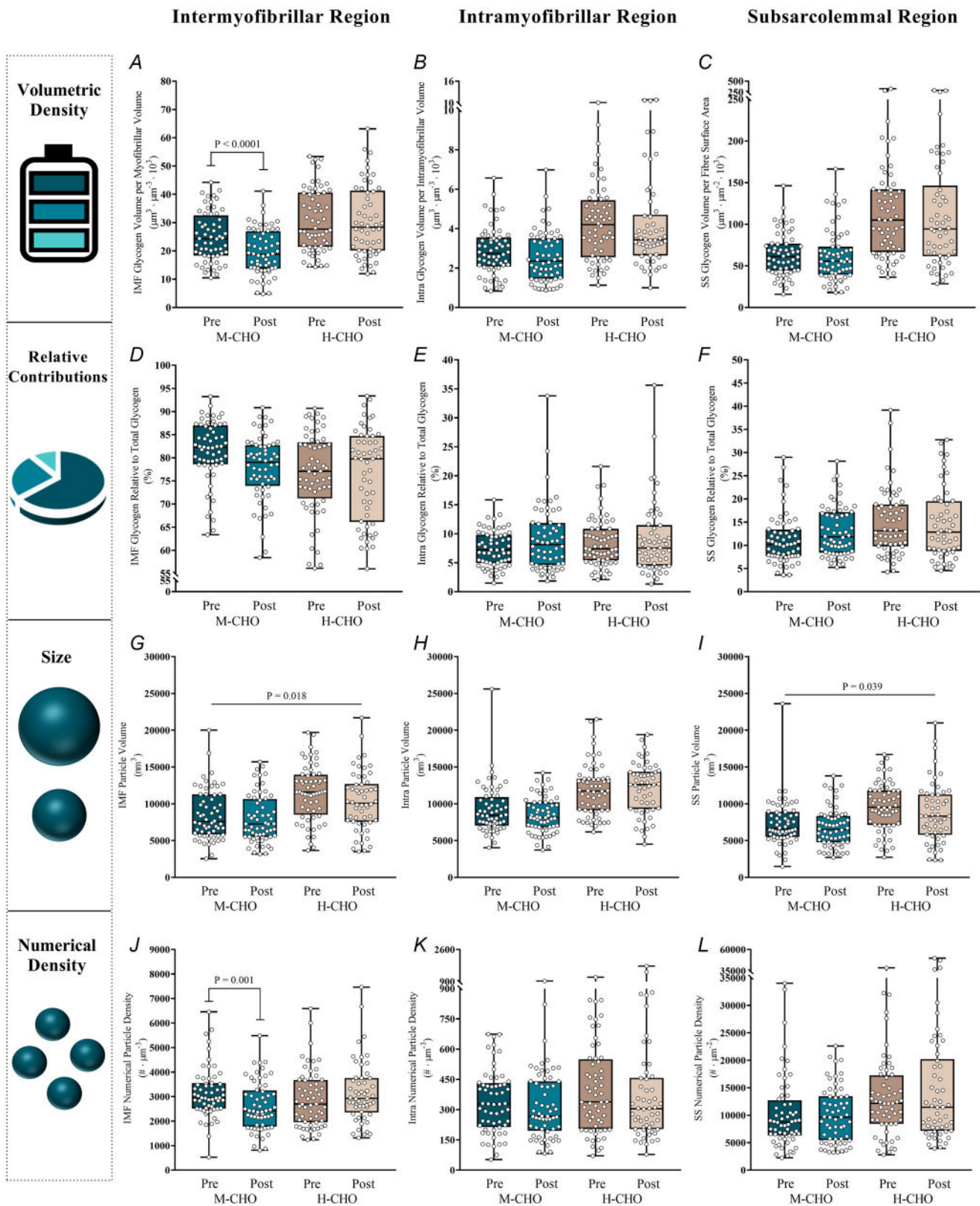


Figure 7. Effects of 1-min maximal cycling exercise on subcellular glycogen utilisation, particle size and numerical density

Values are from biopsies obtained before (pre) and immediately after (post) the 1-min maximal cycling exercise. A–C, glycogen volumetric density; D–F, relative contribution to total glycogen; G–I, particle size; J–L, numerical

particle density. Data shown as median (interquartile range). All individual fibres are displayed as a circle with six fibres from each participant. M-CHO Pre: $n = 60$, Post: $n = 60$, and H-CHO Pre: $n = 60$, Post: $n = 54$. P -values represent main effect of time or pairwise comparisons in case of a time \times diet interaction from linear mixed model. IMF, intermyofibrillar; Intra, intramyofibrillar; SS, subsarcolemmal.

be distributed from subsarcolemmal mitochondria to the intermyofibrillar mitochondria through mitochondrial connectivity (Glancy et al., 2015). Thus, subsarcolemmal glycogen could potentially be a source for mitochondrial pyruvate and facilitate energy transfer by intermyofibrillar mitochondria. Nevertheless, our data suggest that this mechanism was not present under the conditions of the present project, and it can be speculated that the subsarcolemmal mitochondria were inactive during this type of exercise.

Importantly, calculating the expected glycogen utilisation per external work assumes that all energy provided originates from glycogen. Hence, it is presumed that the contribution of creatine phosphate and blood glucose did not differ between the 1-min and 15-min maximal exercise tests. The contribution of creatine phosphate is likely 10%–20% of the total energy consumption during the 1-min test and negligible during the 15-min test (Gastin, 2001). This discrepancy between the tests will mitigate the anticipated decrease in glycogen utilisation during the 15-min maximal exercise in comparison to the 1-min maximal exercise, shifting the estimated value from 0.43 to approximately 0.60. However, this adjustment does not alter the interpretation of the variations in pool-specific glycogen utilisation between the two tests. The assumption about the contribution of blood glucose appears justified, since Katz et al. (1986) found almost no contribution of glucose uptake to the metabolism of the working limb during short-term (~ 5 min) maximal exercise. This is in contrast to exercise of longer durations where blood glucose would make up a larger part of total energy contribution (Romijn et al., 1993), depending on the exogenous supply (Coyle et al., 1986). Interestingly, we have previously found that a 4-h recovery period without energy intake predominantly restricts resynthesis of intramyofibrillar glycogen compared to recovery with CHO intake (Nielsen et al., 2011), which suggest an association between glucose uptake and intramyofibrillar glycogen. Thus, during exercise of longer durations (> 15 min) the glycogen utilisation per external work from the intramyofibrillar pool may decrease due to a larger contribution of blood glucose. In that study subsarcolemmal glycogen was not sensitive to CHO intake, but it can be speculated that the localisation just beneath the sarcolemma makes it sensitive to glucose uptake during prolonged exercise.

Reducing CHO and energy intake after glycogen-depleting exercise mediated smaller pre-exercise glycogen particles

Reducing the amounts of dietary carbohydrates and total energy intake after the glycogen-depleting exercise by the M-CHO diet induced a $\sim 20\%$ – 30% lower glycogen volume density in the subcellular regions than after ingesting the H-CHO diet. This reduction in glycogen content was primarily mediated by a marked reduction in glycogen particle size of $\sim 20\%$ – 30% , whereas the numerical density of glycogen particles was either maintained or reduced $\sim 6\%$ – 21% . Thus, a preservation of the number of glycogen particles per volume seems to be prioritized at the expense of size when storing glycogen under conditions of reduced CHO intake and energy availability.

It is imperative to approach the interpretation of data on particle size and numerical density based on visual inspection of transmission electron micrographs with care, as the smallest particles may not be detectable. As a result, when particles become very small (e.g. due to prolonged exhaustive exercise) it becomes challenging to ascertain any potential decrease in numerical density, and the average particle size may be severely overestimated. In the present study, the particles were reduced in apparent size from around 27 nm to 24 nm in diameter. This range in size is well above a potential detection threshold of 8–12 nm, indicating that the number of undetected particles per volume is expected to be minimal.

Nevertheless, the particle diameter was well below the theoretical maximal of 42 nm across all subcellular localisations and after both diets. This is in line with several studies in human skeletal muscles observing that glycogen particles are stored at a submaximal size (Gejl et al., 2017; Jensen et al., 2021; Marchand et al., 2002, 2007; Nielsen et al., 2012), possibly to balance the need for a readily available fuel store and efficient storage (Shearer & Graham, 2004). This preference for several medium-sized particles also aligns with an indicated occurrence of smaller glycogen particles, but unaltered total glycogen content, observed when over-expressing glycogenin, the glycogen synthesis-priming protein located in the core of the particle (Skurat et al., 1997). Several medium-sized particles also preserve a higher spatial distribution of particles, which could explain the observed down-regulation of glycogen content through the size of particles in the present study.

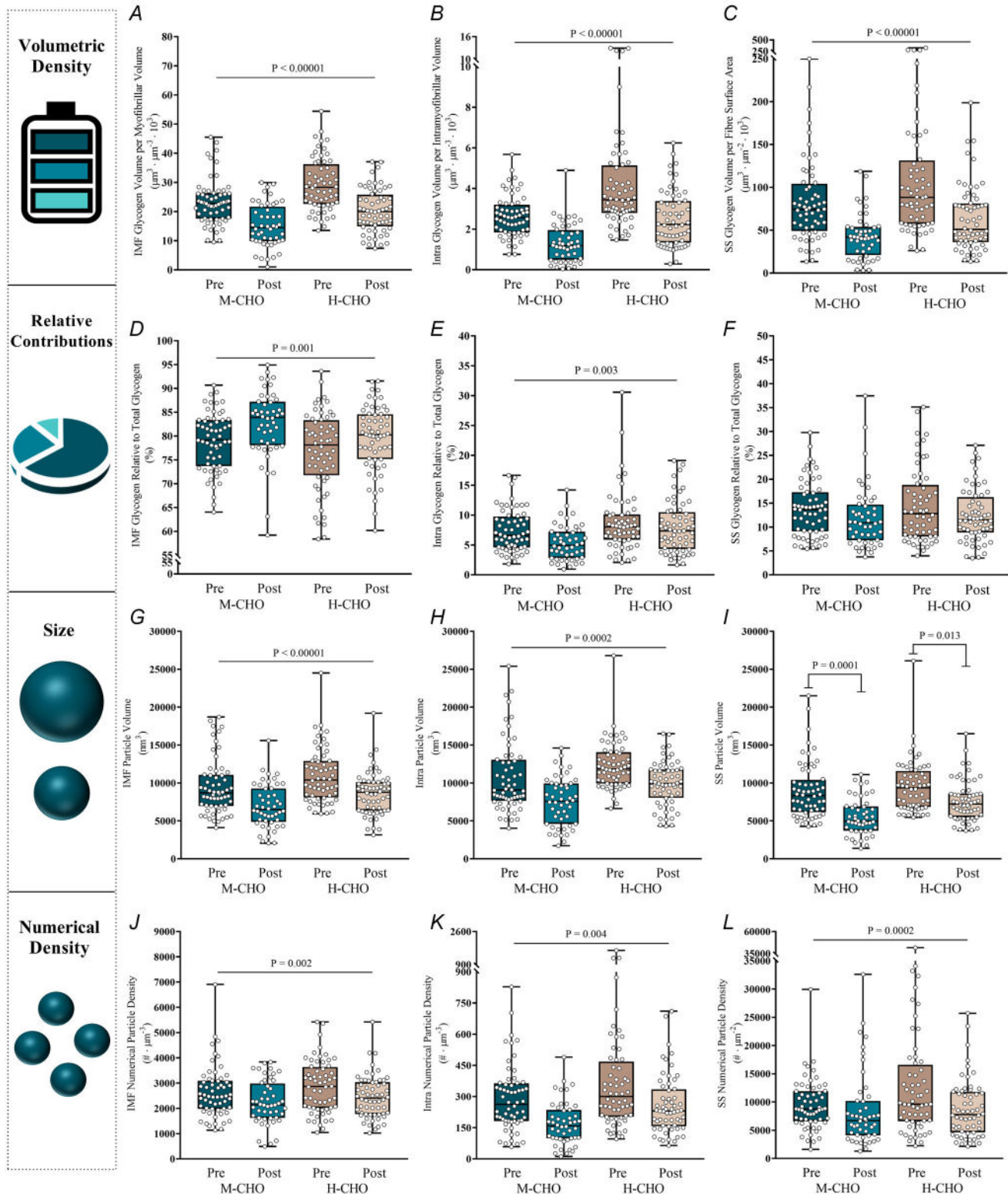


Figure 8. Effects of 15-min maximal cycling exercise on subcellular glycogen utilisation, particle size and numerical density

Values are from biopsies obtained before (pre) and immediately after (post) the 15-min maximal cycling exercise. A–C, glycogen volumetric density; D–F, relative contribution to total glycogen; G–I, particle size; J–L, numerical

particle density. Data shown as median (interquartile range). All individual fibres are displayed as a circle with six fibres from each participant. M-CHO Pre: $n = 60$, Post: $n = 48$, and H-CHO Pre: $n = 60$, Post: $n = 60$. P -values represent main effect of time or pairwise comparisons in case of a time \times diet interaction from linear mixed model. IMF, intermyofibrillar; Intra, intramyofibrillar; SS, subsarcolemmal.

The difference in particle size between the M-CHO and H-CHO diet contrasts with the observations of Jensen et al. (2021). Here, particle sizes were remarkably similar across diets with low, moderate or high amounts of CHO (with low and high CHO conditions consumed after glycogen-depleting exercise), while differences in numerical density primarily accounted for differences in glycogen content. This controversy can be interpreted in two ways: (1) there may exist a broad optimum (~ 23 – 27 nm) for the glycogen particle diameter with respect to metabolic power and storage efficiency, since the density of glycosyl units does not vary to a large degree at submaximal sizes as for small and large particles. Accordingly, the numerical density of glycogen particles is not maintained in the low CHO condition in Jensen et al. (2021) since the diameter of the particles is close to the lower limit in this optimum (i.e. avoiding an unfavourable decrease in particle size with respect to storage efficiency). (2) The diets provided in Jensen et al. (2021) were, contrary to the present study, isocaloric, which could indicate that it is the lower energy intake in the M-CHO than the H-CHO diet of the present study that mediated the reduced particle size, rather than the lower CHO amount *per se*. It remains to be investigated

how energy deficiency affects glycogen particle size and numerical density in different subcellular localisations.

A decreased numerical density of intramyofibrillar and subsarcolemmal glycogen particles (but not intermyofibrillar glycogen particles) was observed, leading to a predominant lowering of the intramyofibrillar and subsarcolemmal glycogen volumetric densities compared with the intermyofibrillar (~ 30 vs. $\sim 20\%$, respectively). This indicates that these two specific pools of glycogen are more sensitive to dietary carbohydrate intake and/or energy availability than intermyofibrillar glycogen, and that a maintenance of intermyofibrillar glycogen is preferred. A preservation of intermyofibrillar glycogen has also been observed during 4 min of maximal exercise (Gejl et al., 2017) and during prolonged exhaustive exercise (Jensen, Ørtenblad, et al., 2020; Nielsen et al., 2011). A differential sensitivity of the distinct pools to carbohydrates and/or energy was also found during a 4-h recovery period, with intermyofibrillar glycogen resynthesis favoured in the absence of carbohydrate and/or energy intake, but intramyofibrillar glycogen resynthesis favoured in the presence of carbohydrate and/or energy intake (Nielsen et al., 2011). In isolated rodent muscles, we have previously found that intermyofibrillar glycogen correlates inversely with half

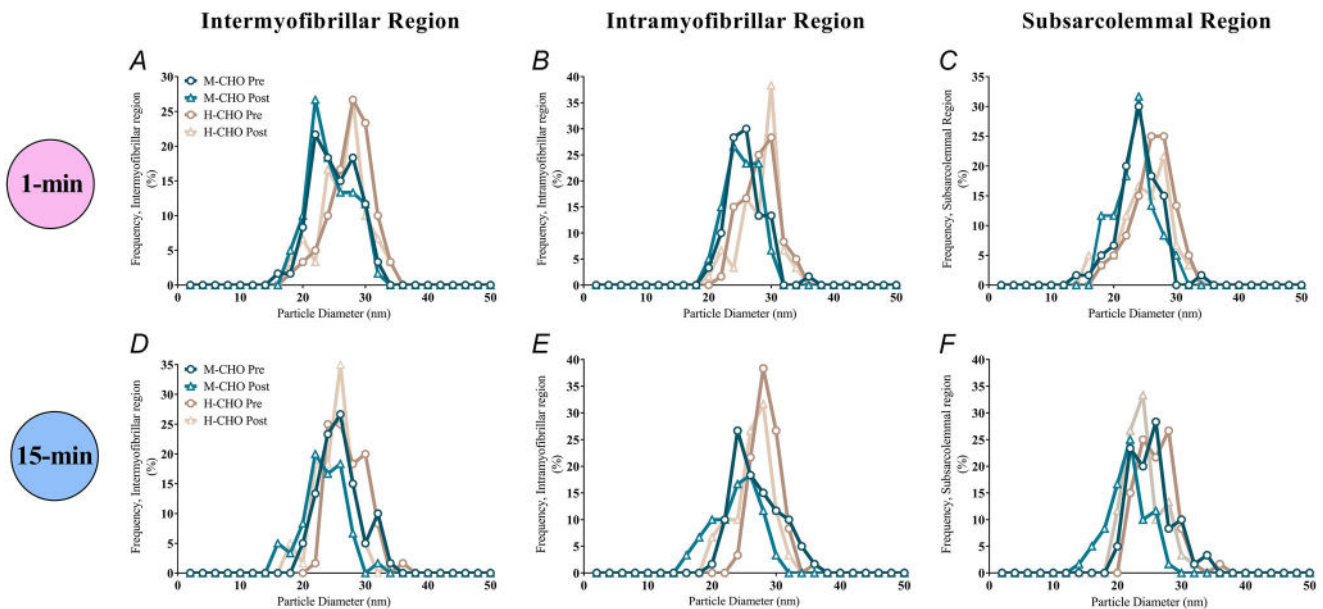


Figure 9. The glycogen particle diameter showed normal distribution

The relative frequency distribution of particle diameter with a bin size of 2 nm in the intermyofibrillar, intramyofibrillar and subsarcolemmal region prior to and after 1-min (A–C) and 15-min (D–F) maximal cycling exercise after adhering to the M-CHO or H-CHO diet. M-CHO Pre: $n = 60/60$ (1-min/15-min), Post: $n = 60/48$, H-CHO Pre: $n = 60/60$, and Post: $n = 54/60$.

tetanic relaxation time (Nielsen et al. 2009) and that intermyofibrillar glycogen is the only pool of glycogen, which fuels the SR Ca^{2+} -ATPase (Nielsen et al., 2022). Thus, several studies suggest a preservation of intermyofibrillar glycogen, and this may be a safety mechanism by maintaining a ready energy availability for the SR Ca^{2+} -ATPase, and securing re-uptake of Ca^{2+} into the SR and thereby prevent damaging cytosolic Ca^{2+} accumulation (Duncan & Smith, 1978; Turner et al., 1988).

Reducing CHO and energy intake after glycogen-depleting exercise did not affect utilisation during the 1- and 15-min maximal exercise

Lastly, we investigated how the different storage of glycogen between the H-CHO and M-CHO conditions, in terms of glycogen particle size and numerical density, was affected during maximal cycling exercise. In general, it seemed that the pattern of both a decrease in particle size and numerical density was not affected by smaller particles in the M-CHO condition. Previously, we have examined the glycogen particle size before and after 4 min of maximal exercise after ingesting a diet with a high amount of CHO for 24 h (Gejl et al., 2017). Here, the average glycogen volumetric density declined more than the glycogen particle volume, indicating that also in this study the utilisation of glycogen can be ascribed to a decrease in both particle size and numerical density. We suggest that due to the rather small difference in particle size (~ 24 vs. ~ 27 nm), and, in turn, expected small difference in glycosyl unit density per particle (Melendez et al., 1998; Shearer & Graham, 2004) between the M-CHO and H-CHO conditions of the present study, the utilisation pattern (size vs. numerical density) was not affected by differences in pre-exercise particle volume and numerical density.

We observed an effect of the diet intervention on the utilisation of intermyofibrillar glycogen during the 1-min maximal exercise. However, since intermyofibrillar glycogen comprises approximately 80% of total glycogen and this effect is not corroborated by the biochemically determined glycogen content, we interpret that the utilisation of intermyofibrillar glycogen (as with intramyofibrillar and subsarcolemmal glycogen) was not influenced by the diet intervention.

Concluding remarks

We utilised TEM and standard stereological techniques to quantify the volumetric density of skeletal muscle glycogen within three distinct subcellular pools. Biopsies were extracted from young males subjected to either 1 or 15 min of maximal ergometer cycling exercise. Our analysis revealed divergent preferences

for glycogen storage pools during the two exercise durations. Specifically, 1 min of maximal exercise predominantly depleted intermyofibrillar glycogen, whereas 15 min of maximal exercise primarily targeted intramyofibrillar glycogen. As exercise duration extends from 1 to 15 min, the relative energy contribution from aerobic metabolism to total energy turnover is markedly higher. The findings from this investigation propose that the degradation rate of glycogen ceases exclusively for intermyofibrillar glycogen when transitioning from 1-min to 15-min maximal exercise, while the degradation rate of intramyofibrillar and subsarcolemmal glycogen remains elevated. If substantiated, these results indicate that regulation of glycogenolytic rate during exercise is dependent on the subcellular localisation in human skeletal muscle fibres. Also, we here reveal that a lowering of dietary carbohydrates and energy after glycogen-depleting exercise decreased glycogen availability by inducing a smaller glycogen particle size across all subcellular pools, while the numerical density was lower in the intramyofibrillar and subsarcolemmal pools. It is noteworthy that this disparate storage pattern had no effect on the subsequent utilisation during the maximal cycling exercises.

References

- Bishop, D., Bonetti, D., & Spencer, M. (2003). The effect of an intermittent, high-intensity warm-up on supramaximal kayak ergometer performance. *Journal of Sports Sciences*, **21**(1), 13–20.
- Coyle, E. F., Coggan, A. R., Hemmert, M. K., & Ivy, J. L. (1986). Muscle glycogen utilization during prolonged strenuous exercise when fed carbohydrate. *Journal of Applied Physiology*, **61**(1), 165–172.
- Duncan, C. J., & Smith, J. L. (1978). The action of caffeine in promoting ultrastructural damage in frog skeletal muscle fibres. Evidence for the involvement of the calcium-induced release of calcium from the sarcoplasmic reticulum. *Naunyn-Schmiedeberg's Archives of Pharmacology*, **305**(2), 159–166.
- Dutka, T. L., & Lamb, G. D. (2007). Na^+ - K^+ pumps in the transverse tubular system of skeletal muscle fibers preferentially use ATP from glycolysis. *American Journal of Physiology-Cell Physiology*, **293**(3), C967–C977.
- Essén, B. (1978). Glycogen depletion of different fibre types in human skeletal muscle during intermittent and continuous exercise. *Acta Physiologica Scandinavica*, **103**(4), 446–455.
- Gastin, P. B. (2001). Energy system interaction and relative contribution during maximal exercise. *Sports Medicine*, **31**(10), 725–741.
- Gejl, K. D., Hvid, L. G., Frandsen, U., Jensen, K., Sahlin, K., & Ørtenblad, N. (2014). Muscle glycogen content modifies SR Ca^{2+} release rate in elite endurance athletes. *Medicine and Science in Sports and Exercise*, **46**(3), 496–505.

- Glancy, B., Hartnell, L. M., Malide, D., Yu, Z. X., Combs, C. A., Connelly, P. S., Subramaniam, M., & Subramaniam, S. (2015). Mitochondrial reticulum for cellular energy distribution in muscle. *Nature*, **523**, 617–620.
- Gejl, K. D., Ørtenblad, N., Andersson, E., Plomgaard, P., Holmberg, H. C., & Nielsen, J. (2017). Local depletion of glycogen with supramaximal exercise in human skeletal muscle fibres. *The Journal of Physiology*, **595**(9), 2809–2821.
- Goldsmith, E., Sprang, S., & Fletterick, R. (1982). Structure of maltoheptaose by difference Fourier methods and a model for glycogen. *Journal of Molecular Biology*, **156**(2), 411–427.
- Gunja-Smith, Z., Marshall, J. J., Mercier, C., Smith, E. E., & Whelan, W. J. (1970). A revision of the Meyer-Bernfeld model of glycogen and amylopectin. *FEBS Letters*, **12**(2), 101–104.
- Hargreaves, M., & Spriet, L. L. (2018). Exercise metabolism: Fuels for the fire. *Cold Spring Harbor Perspectives in Medicine*, **8**(8), a029744.
- Howard, C. V., & Reed, M. G. (2005). *Unbiased Stereology. Three-Dimensional Measurement in Microscopy*. Bios Scientific.
- James, J. H., Wagner, K. R., King, J. K., Leffler, R. E., Upputuri, R. K., Balasubramaniam, A., Friend, L. A., Shelly, D. A., Paul, R. J., & Fisher, J. E. (1999). Stimulation of both aerobic glycolysis and Na(+)-K(+)-ATPase activity in skeletal muscle by epinephrine or amylin. *American Journal of Physiology*, **277**(1), E176–E186.
- Jensen, R., Nielsen, J., & Ørtenblad, N. (2020). Inhibition of glycogenolysis prolongs action potential repriming period and impairs muscle function in rat skeletal muscle. *The Journal of Physiology*, **598**(4), 789–803.
- Jensen, R., Ørtenblad, N., di Benedetto, C., Qvortrup, K., & Nielsen, J. (2022). Quantification of subcellular glycogen distribution in skeletal muscle fibers using transmission electron microscopy. *Journal of Visualized Experiments* (180). <https://doi.org/10.3791/63347>
- Jensen, R., Ørtenblad, N., Stausholm, M. H., Skjærbæk, M. C., Larsen, D. N., Hansen, M., Holmberg, H. C., Plomgaard, P., & Nielsen, J. (2020). Heterogeneity in subcellular muscle glycogen utilisation during exercise impacts endurance capacity in men. *The Journal of Physiology*, **598**(19), 4271–4292.
- Jensen, R., Ørtenblad, N., Stausholm, M. H., Skjærbæk, M. C., Larsen, D. N., Hansen, M., Holmberg, H. C., Plomgaard, P., & Nielsen, J. (2021). Glycogen supercompensation is due to increased number, not size, of glycogen particles in human skeletal muscle. *Experimental Physiology*, **106**(5), 1272–1284.
- Katz, A., Broberg, S., Sahlin, K., & Wahren, J. (1986). Leg glucose uptake during maximal dynamic exercise in humans. *American Journal of Physiology*, **251**(1 Pt 1), E65–E70.
- Lin, L. I.-K. (1989). A concordance correlation coefficient to evaluate reproducibility. *Biometrics*, **45**(1), 255–268.
- Madsen, N. B., & Cori, C. F. (1958). The binding of glycogen and phosphorylase. *Journal of Biological Chemistry*, **233**(6), 1251–1256.
- Marchand, I., Chorneyko, K., Tarnopolsky, M., Hamilton, S., Shearer, J., Potvin, J., & Graham, T. E. (2002). Quantification of subcellular glycogen in resting human muscle: Granule size, number, and location. *Journal of Applied Physiology*, **93**(5), 1598–1607.
- Marchand, I., Tarnopolsky, M., Adamo, K. B., Bourgeois, J. M., Chorneyko, K., & Graham, T. E. (2007). Quantitative assessment of human muscle glycogen granules size and number in subcellular locations during recovery from prolonged exercise. *The Journal of Physiology*, **580**(Pt. 2), 617–628.
- Medbø, J. I., Mohn, A. C., Tabata, I., Bahr, R., Vaage, O., & Sejersted, O. M. (1988). Anaerobic capacity determined by maximal accumulated O₂ deficit. *Journal of Applied Physiology*, **64**(1), 50–60.
- Melendez, R., Melendez-Hevia, E., Mas, F., Mach, J., & Cascante, M. (1998). Physical constraints in the synthesis of glycogen that influence its structural homogeneity: A two-dimensional approach. *Biophysical Journal*, **75**(1), 106–114.
- Melendez-Hevia, E., Waddell, T. G., & Shelton, E. D. (1993). Optimization of molecular design in the evolution of metabolism: The glycogen molecule. *Biochemical Journal*, **295**(Pt 2), 477–483.
- Nielsen, J., Cheng, A. J., Ørtenblad, N., & Westerblad, H. (2014). Subcellular distribution of glycogen and decreased tetanic Ca²⁺ in fatigued single intact mouse muscle fibres. *The Journal of Physiology*, **592**(9), 2003–2012.
- Nielsen, J., Dubillot, P., Stausholm, M. H., & Ørtenblad, N. (2022). Specific ATPases drive compartmentalized glycogen utilization in rat skeletal muscle. *Journal of General Physiology*, **154**(9), e202113071.
- Nielsen, J., Holmberg, H. C., Schröder, H. D., Saltin, B., & Ørtenblad, N. (2011). Human skeletal muscle glycogen utilization in exhaustive exercise: role of subcellular localization and fibre type. *The Journal of Physiology*, **589**(Pt 11), 2871–2885.
- Nielsen, J., Krstrup, P., Nybo, L., Gunnarsson, T. P., Madsen, K., Schröder, H. D., Bangsbo, J., & Ørtenblad, N. (2012). Skeletal muscle glycogen content and particle size of distinct subcellular localizations in the recovery period after a high-level soccer match. *European Journal of Applied Physiology*, **112**(10), 3559–3567.
- Nielsen, J., Schröder, H. D., Rix, C. G., & Ørtenblad, N. (2009). Distinct effects of subcellular glycogen localization on tetanic relaxation time and endurance in mechanically skinned rat skeletal muscle fibres. *The Journal of Physiology*, **587**(Pt 14), 3679–3690.
- Ovadi, J., & Saks, V. (2004). On the origin of intracellular compartmentation and organized metabolic systems. *Molecular and Cellular Biochemistry*, **256–257**(1–2), 5–12.
- Romijn, J. A., Coyle, E. F., Sidossis, L. S., Gastaldelli, A., Horowitz, J. F., Endert, E., & Wolfe, R. R. (1993). Regulation of endogenous fat and carbohydrate metabolism in relation to exercise intensity and duration. *American Journal of Physiology*, **265**(3 Pt 1), E380–E391.
- Schytz, C. T., Ørtenblad, N., Birkholm, T. A., Plomgaard, P., Nybo, L., Kolnes, K. J., Andersen, O. E., Lundby, C., Nielsen, J., & Gejl, K. D. (2023). Lowered muscle glycogen

- reduces body mass with no effect on short-term exercise performance in men. *Scandinavian Journal of Medicine & Science in Sports*, **33**(7), 1054–1071.
- Shearer, J., & Graham, T. E. (2004). Novel aspects of skeletal muscle glycogen and its regulation during rest and exercise. *Exercise and Sport Sciences Reviews*, **32**(3), 120–126.
- Sjöström, M., Ångquist, K. A., Bylund, A. C., Fridén, J., Gustavsson, L., & Scherstén, T. (1982). Morphometric analyses of human muscle fiber types. *Muscle & Nerve*, **5**(7), 538–553.
- Sjöström, M., Kidman, S., Larsén, K. H., & Ångquist, K. A. (1982). Z- and M-band appearance in different histochemically defined types of human skeletal muscle fibers. *Journal of Histochemistry and Cytochemistry*, **30**(1), 1–11.
- Skurat, A. V., Lim, S. S., & Roach, P. J. (1997). Glycogen biogenesis in rat 1 fibroblasts expressing rabbit muscle glycogenin. *European Journal of Biochemistry*, **245**(1), 147–155.
- Thomas, D. T., Erdman, K. A., & Burke, L. M. (2016). American college of sports medicine joint position statement. nutrition and athletic performance. *Medicine and Science in Sports and Exercise*, **48**(3), 543–568.
- Turner, P. R., Westwood, T., Regen, C. M., & Steinhardt, R. A. (1988). Increased protein degradation results from elevated free calcium levels found in muscle from mdx mice. *Nature*, **335**(6192), 735–738.
- Verkman, A. S. (2002). Solute and macromolecule diffusion in cellular aqueous compartments. *Trends in Biochemical Sciences*, **27**(1), 27–33.
- Vigh-Larsen, J. F., Ortenblad, N., Emil Andersen, O., Thorsteinsson, H., Kristiansen, T. H., Bilde, S., Mikkelsen, M. S., Nielsen, J., Mohr, M., & Overgaard, K. (2022). Fibre type- and localisation-specific muscle glycogen utilisation during repeated high-intensity intermittent exercise. *The Journal of Physiology*, **600**(21), 4713–4730.
- Wanson, J. C., & Drochmans, P. (1968). Rabbit skeletal muscle glycogen. A morphological and biochemical study of glycogen beta-particles isolated by the precipitation-centrifugation method. *Journal of Cell Biology*, **38**(1), 130–150.
- Weibel, E. R. (1980). *Stereological Methods* (vol. 2). Theoretical Foundations. Academic Press.

Additional information

Data availability statement

The data that support the findings of this study are available from the corresponding author upon reasonable request.

Competing interests

The authors declare no conflict of interest.

Author contributions

C.T.S., K.D.G., N.Ø. and J.N. contributed to the conception and design of the experiments. All authors contributed to the data collection, analyses and/or data interpretation. C.T.S. and J.N. drafted the manuscript, while all authors edited and/or revised the manuscript. The final version of the manuscript was approved by all authors, and all agree to be accountable for all aspects of the work in ensuring that questions related to the accuracy or integrity of any part of the work are appropriately investigated and resolved. All persons stated as authors qualify for authorship, and all those who qualify for authorship are listed.

Funding

The present study was supported by Team Denmark by means from the Novo Nordisk Foundation to the Danish Elite Endurance Performance Network; The Danish Ministry of Culture (FPK.2020-0042); and Swedish Olympic Committee.

Acknowledgements

The authors thank Dorte Mengers Flindt, Chris Christensen, Mikkel Egeskov Vigen, and Martin Harris Larsen for technical assistance. The imaging by transmission electron microscopy was performed at the Core Facility for Integrated Microscopy, Faculty of Health and Medical Science, University of Copenhagen.

Keywords

carbohydrate, fatigue, high-intensity exercise, performance, skeletal muscle fibres, subcellular glycogen, transmission electron microscopy

Supporting information

Additional supporting information can be found online in the Supporting Information section at the end of the HTML view of the article. Supporting information files available:

Peer Review History